Leveraging on Green Energy Harvesting via Dye Sensitized Solar Cells; Their Components, Operations and Graphene Based Electrodes

Authors

Njeru, Elosy Gatakaa[1*], Muasya Alex Njoroge[2], Kamweru Paul Kuria[3], Gichumbi Joel Mwangi[4]

Department of Physical sciences, Faculty of Science Engineering and Technology, Chuka University, Kenya

*Corresponding Author

Njeru, Elosy Gatakaa

Abstract

One possible technological development in solar cells is thought to be dye-sensitized solar cells (DSSCs). The energy-producing method employed by DSSCs is similar to that of plant cells and is based on the photo-electrochemical moments of electrons that are brought about by the interaction of photon energy and chemical reaction. Synthetic dyes that are employed as sensitizers in DSSCs have higher efficiency and longer endurance, but they also have drawbacks such the use of rare metallic components that are vulnerable to environmental degradation. As a result, researchers are experimenting with natural alternative sensitizers that are biocompatible. Plant pigments like carotenoids, flavonoids, anthocyanins, and chlorophyll are in charge of the chemical reactions in these natural sensitizers. Therefore, it is relatively easy to extract dyes containing this pigment from natural sources such as flowers, seeds, and leaves, among others. The structure and functioning of DSSCs are the main topics of this review. This review focuses on the structure and operations of DSSCs. Components of DSSCs photosensitizers, photo-anodes and counter electrodes and their functions have been outlined. Detailed summary of synthetic dye based DSSCs carried out by different groups, have also been reviewed. Details of numerous plant pigments found in plant-based products that are employed as sensitizers in DSSCs have been collated and explained. Open circuit voltage (V_{oc}), short circuit current (I_{sc}), fill factor (FF), and efficiency (η) based on both synthetic and natural dye have also been reported as DSSC performance metrics. Leveraging on the photosensitizers and maximizing on the working electrodes and counter electrodes, DSSCs would serve as the best alternative to meet the world energy demand.

Keywords: *photosensitizer, natural dye, synthetic dye, photoanode, counter electrode, electrolyte*

1.1. Introduction to Solar Cells

Increased growth in human population has led to increased need for consumption of energy in various form[1],[2]. Non-renewable energy sources like natural gases, coal, and petroleum are exhaustible and unsustainable[3],[4]. Furthermore, these non-renewable sources are carbon–based fossil fuels which emit greenhouse gases resulting to global warming posing great danger to the world as well as human beings. Seventy five percent of world's total energy is obtained from non-renewable sources of energy which cannot be

recycled and leads to environmental pollution[5]. This has aroused more research to be focused on renewable energy-based conversion devices. Renewable energy resources available include biomass, solar, wind, hydroelectric, ocean energy among others. Among these resources, solar energy is important since it is available throughout and inexhaustible in nature. Radiation harnessed from sunlight, produces heat and light causing photochemical reaction that generate electricity [6]. Approximately 3.8 EJ of energy are provided when sunlight strikes the earth's surface and this can meet the energy demand for the whole world for one year [7].

Though the sun provides over 10,000 times more energy than world's requirement[8], expensive technologies are involved in its conversion and storage. Scientists have been exploring various techniques of solar energy harvesting since 18th century with the aim to have a simple conversion device. In 1839, Edmond Becquerel discovered the photovoltaic (PV) phenomenon while looking for a practical way to gather solar energy.

In an effort to seek an effective method of solar harvesting, the photovoltaic (PV) effect was discovered by Edmond Becquerel in 1839[5].

Solar photovoltaics (PV), converts light energy from the sun to electricity via photovoltaic effect, using a p-n semiconductor junction device[9], [10]. The combination of the n-doped and p-doped is depicted in Figure 1. When the n-doped layer is exposed to radiation, the excited electrons travel to the conduction band. Following the circuit, they enter through an external circuit and reach the p-doped layer. The energy levels will cause the electrons to once more shift to the n-type layer.
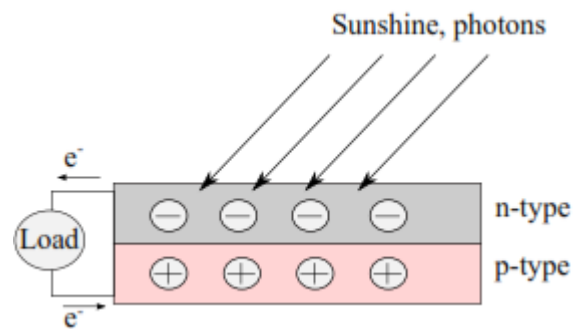
Figure 1: A silicon (Si) solar cell schematically illustrated [9].

1.1.1. Generations of Solar Cells

Three generations can be distinguished in photovoltaic technology. The various classifications of solar cell technologies are shown in Figure 2. The first generation was produced on Si wafers. This generation of solar cells is of two types namely: the single (mono) crystalline solar cells and the multi (poly) crystalline solar cells. Czochralski process is used to manufacture the mono crystalline solar cell [11]. The Si crystals are cut from the big sized Si ingots. Polycrystalline PV modules have various crystals, all of them put together in one single cell [10]. Polycrystalline Si solar cells are more affordable than single-crystalline cells because of their manufacturing process, which involves chilling a graphite mold that contains molten silicon to generate various crystal forms.[12]. This makes polycrystalline modules to be cheaper in fabrication compared to monocrystalline modules but at the same time their efficiency is slightly compromised. Some of the undoing's of the first generation, and has led to a continuous search for better solar cells includes the Shockley- Queisser limit which affects the performance of silicon solar cells (discussed in section 1.1.2.) and a high cost of production due to the high demand for energy during the purification of silicon. Through continued research, more economical second generation of solar cells have been developed [13].
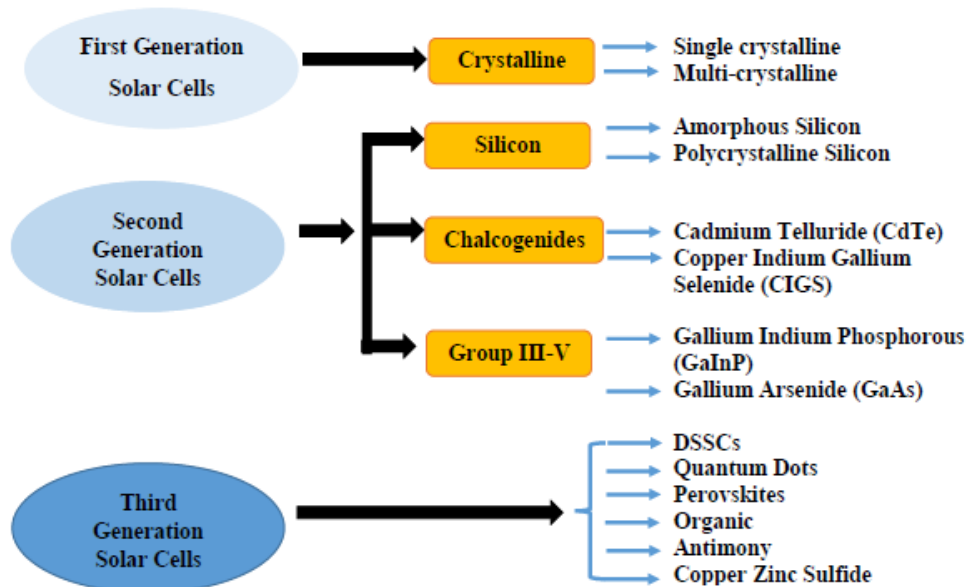
Figure 2: Classification of solar cell

Materials used in second-generation includes indium tin oxide (t-Si), amorphous silicon (a-Si), and cadmium indium selenide (CIS)[14]. Thin-layered solar cells are produced at low temperatures with the integration of cell insulation and a high degree of automation in order to lower the cost of solar cell manufacture. Thin layer technology uses flexible substrates. This property enables these cells to be of great use in energy conversion sectors while opening other areas of applications such as textile industries[15]. Although thin film solar cells are of great use, they have limited stability as they suffer from Staebler-Wronski effect which is the initial degradation experienced by solar cells when exposed to outdoor conditions resulting to low power conversion efficiency as can be seen in Figure 18.

With efficiency above 25%, the second generation of solar cells has been the most successful generation. Amorphous silicon, micromorphous silicon, copper indium gallium diselenide, and cadmium telluride (CdTe) are a few of the materials that have been adopted frequently in this generation. Other materials includes the Group III-V semiconductors have been used to produce solar cells and registered highest efficiencies in any photovoltaic technology so far. Examples of these materials are Gallium Indium Phosphorous (GaInP) and Gallium Arsenide (GaAs). For instance, a thin sheet of cadmium telluride (CdTe) in a cadmium telluride solar cell absorbs sunlight and turns it into energy. In comparison to CIGS and A-Si technologies, CdTe technology costs 30% less[16], making it to be more popular but has the downside that cadmium is toxic if released to environment. Other direct band gap materials that have been employed includes the Copper indium gallium selenide (CIGS) which have attained the highest efficiency of (~20%) among thin film materials. The amorphous photovoltaic cell is usually made of a p-i-n junction with a microcrystalline silicon. The amorphous silicon cells have gained a lot of popularity due to the various advantages over the CdTe counterparts which includes:-

1. It uses nontoxic materials when compared to the CdTe cells making it safe for human use and environmentally friendly,

2. The processing temperature of these devices is usually low and this makes it possible for the production of these devices to take place on glass substrates,

3. It uses glass substrates that are of low cost and flexible.

The above mentioned advantages of the amorphous silicon solar cells has made it to gain a

lot of popularity over the CdTe solar cells[17]. The photo electrically active material of amorphous silicon made of a very thin layer of which makes it have a high rate of light absorption compared to the other crystalline cells. However, due to its amorphous nature, high levels of inherent disorder, and dangling links, it performs poorly as a conductor for charge carriers. Amorphous silicon has a band gap energy of 1.7 eV, which is larger than that of crystalline silicon's 1.0 eV, and is primarily responsible for light absorption in the visible portion of the solar spectrum[18].

Third-generation technologies have been developed and are continuously being investigated in an effort to enhance the electrical performance of the second generation of solar cells while still reducing the cost of production. The mode of operation of these cells is different from all the others since they do not require the p-n junction that is traditionally used by the other semiconductor silicon cells. Additionally, this generation has a wide application in polymer solar cells[19], nanocrystalline cells, and dye-sensitized solar cells (DSSCs) [20].

DSSCs have gained a lot of interest and researchers are continually inventing new ways of improving their performance. Use of new dyes that are ecofriendly, variation of the choice of the electrolyte and maximizing on the electrodes by trying different photo anodes and counter electrodes are some of the areas of interest. For example,[21], co-sensitized alkoxysilyl-anchor and carboxy-anchor organic dyes and reported an improvement of PCE of up to 4.53 %.

1.1.2.   Shockley-Queisser Limit (SQ)

Initially, [22] estimated the (SQ) limit by equating the photon fluxes entering and leaving a device under open circuit. A theoretical framework based on the concept of precise balancing was used to determine a single junction's solar cell limiting efficiency[23]. A graph of efficiency against bandgap energy of a single junction cell is illustrated in Figure 3 and lists a few semiconductors that are commonly utilized in second-generation photovoltaics.
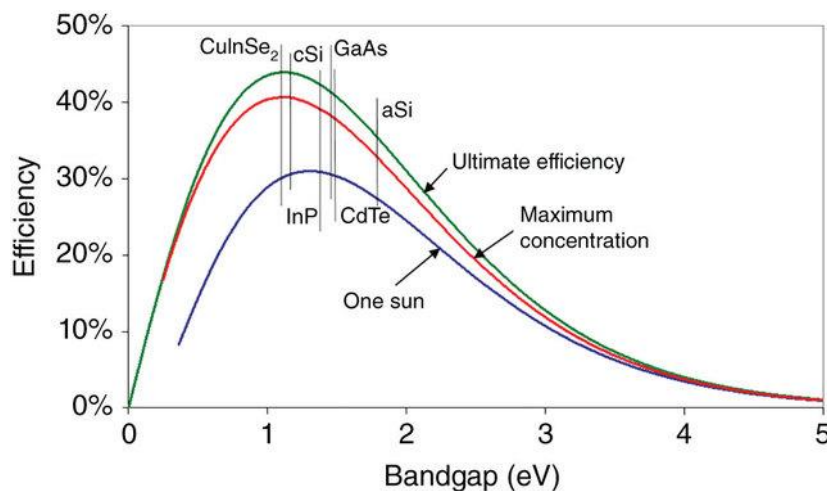
Figure 3: The bandgaps of the semiconductors CuInSe2, InP, cSi, GaAs, CdTe, and aSi that are usable in second generation photovoltaics. At temperatures of 6000 K for the incident light beam and 300 K for the emission, the black-body spectrum is present. Figure obtained from [22].

In search for highly efficient solar cell candidates, materials that are good absorbers and radiators are required[23]. Evaluation of solar cell is done basing on two properties; strength of light absorption and

secondly, whether the created charge carriers reach the electrical contact successfully[24]. Photon dynamics are important to be engineered in high efficiency solar cell. About 100% external

luminescence is required for SQ limit so as to balance the incoming sunlight at open circuit. The SQ model integrates different methods for controlling and capturing light, including photon recycling, optical concentration, and emission angle restriction. When photons with a larger band gap energy impact the surface of a semiconductor, they release photons with a lower energy, creating electron-hole pairs[25]. The produced carriers must all be collected as current in the leads or recombined, generating one photon for each pair of electron-hole pairs, in order to achieve the highest possible cell efficiency[26]. Another way of improving solar cells' efficiency to nearly attaining the SQ limit is by Substitution of Cu+ with Ag+[27].

Fundamental and technical limitations are experienced in search of efficient low cost solutions for the solar energy conversion[28]. Fundamental limitations, also known as intrinsic limitations, are losses resulting from the PV cell's inability to utilize photons with energies below the band gap [29], [30], thermalization of charge carriers, which results from the absorption of photons with energies above the band gap of the PV material [31], [32], and losses resulting from the recombination of the light-generated charge carriers[32], [33]. Technical limitations also known as extrinsic limitations such as low absorption efficiency of the PV material, can be enhanced by ensuring that the cell is properly designed [34].

Approaches such as combining the incoming radiations into propagating modes within the cell texturing and randomly texturing the surface of the cell improves extrinsic limitations [35]. Despite modifying PV cell, even the ideal one have a maximum intrinsic efficiency of 33 % [29], for the standard solar illumination of 1000 W/m2 and air mass of 1.5 G energy spectrum [36]. Continued research approaches have developed designs that go beyond the S-Q limit for single junction PV cells [28]. These approaches include; intermediate–band and engineering multiple junction solar cell which aids in elimination of thermalization losses [37]. Research has revealed that the intrinsic

thermodynamic efficiency limit can be raised by down converting a high-energy photon into two or more lower-energy photons, which reduces thermalization losses [38], [39].

Another strategy for creating very effective solar energy converters with a theoretical efficiency limit of over 85% involves coupling thermal and photovoltaic converters [40]. The utmost efficiency, though, can only be achieved in unfeasible circumstances, such as temperatures above 2500 K, maximum optical concentration, an infinite ratio of the intermediate absorber's emitting to absorbing surface area, and a narrow band transmission filter[41]. The aforementioned conditions force all the suggested designs to rely on three key elements: a large emitter to absorber area ratio, high operating temperatures of about 2000 K, and a high level of optical concentration.[42].

The efficiency limit of PV cells especially those with large bandgaps can be improved through electronic up-conversion of low energy photon [43]. This method uses a lower-lying metastable state to sequentially excite a PV cell semiconductor. Theoretically, efficiency of the ideal up-conversion enhanced PV cell can reach 63 % [44]. Commonly, used-up convey systems have limiting factors such as low absorption efficiencies and high non-radiative recombination rates [45]. Recently, studies on broadband up-conversion have shown some promising efficiency improvement [46]. The SQ limit maximizes the efficiency of a single p-n junction solar cell with a band gap of 1.1 eV, using AM 1.5 solar spectrum to about 30% [47], see Figure 3.

1.2. Introduction to Dye sensitized solar cells (DSSCs)

Due to their ease of manufacture and high power conversion efficiency, dye-sensitive solar cells (DSSCs), which are third-generation solar cells, are the most potential silicon solar cell substitutes [20]. The first dye sensitized nanocrystalline solar cell was built by [48]. This led to a remarkable progress in solar cell invention with a

photoelectric energy conversion of 7.1%[8]. The research on DSSCs as an alternative source of energy is increasingly becoming more popular over the expensive silicon solar cells. DSSCs uses a relatively cost-effective method of production and although its efficiency is relatively low compared to the silicon solar cells, it's easy to fabricate[49]. Additionally, DSSCs rides over the crystalline silicon cells due to their high sensitivity to the visible light and light that is incident at shallow angles[50]. Therefore, in areas that receive low light intensities, DSSCs would be an ideal power source[8]. DSSCs employs a photo-electrochemical process that imitates the concept of plants photosynthesis. The basic component of a DSSC includes the photo anode which is covered by a dye sensitizer. In a DSSC, the dye sensitizer absorbs light, yielding charge carriers that are subsequently transferred to the wide band gap nanocrystalline semiconductor.

1.3. Structure of the DSSCs

In terms of design and functionality, DSSCs are very different from conventional solar cell technologies. Typical DSSC configurations combine liquid and solid phases [51]. The configuration of a DSSCs typically includes two transparent glass substrates which serves as the electrodes (the photo anode and the counter electrode), onto which a conductive oxide layer of either fluorine-doped tin-oxide or indium-doped tin oxide has been deposited. The photo anode is made of a mesoporous semiconductor metal-oxide of either TiO_2 or ZnO layer is immersed in a dye where a monolayer of dye molecules are adsorbed. Standard practice calls for coating the counter electrode with platinum and injecting an electrolyte comprising a redox pair of iodide/tri-iodide electrolyte between the photo anode and the counter electrode.[1], [6], [51], [52]. The specifications and purposes of each component, which are schematically depicted in Figure 4 are highlighted in Table 1.

Table 1: specification and functions of DSSCs component

Component	Specification	References
Transparent conducting glass (Substrate)	Made up of plastic or glass substrate. Its transparency enables solar rays to be absorbed by the photo anode. The photoanode and the counter electrode conductive materials are deposited on its surface. Provides good electrical conductivity while serving as a current collector. Mostly used TCO substrates include F-doped or In-doped tin oxide and aluminium –doped zinc oxide.	[53], [54]
Mesoporous photoanode	Comprises of a semiconductor metal oxide that provide surface area for dye adsorption.	[5], [54]–[57]
Dye sensitizer	Stimulated as a result of absorbing the sunlight. Some of the frequently used photosensitizers includes: Ru-based sensitizers, metal-free organic sensitizers and natural sensitizers.	[5], [54], [57], [57]
Electrolyte	Redox couple salt that is injected between photo anode and the counter electrode. Its main work is to regenerate the oxidized dye. Inorganic ionic liquids composed of salts or salt mixtures, I-/I-3_in organic solvents, and solid electrolytes like spiro-meotad are all frequently used electrolytes.	[58]
Counter electrode (CE)	It is a thin layer of catalyst material, usually platinum, that has been placed over a substrate made of transparent conductive glass.	[59], [60]
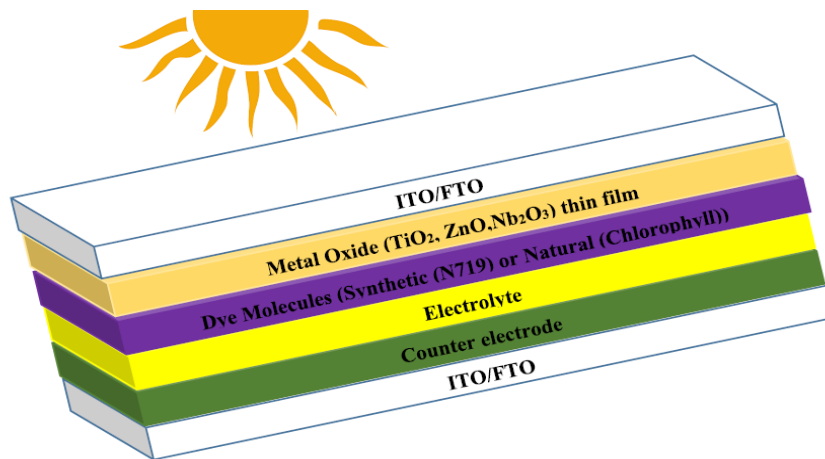
Figure 4: Schematic diagram of a dye sensitized solar cell structure

1.4. Operation of DSSCs

DSSCs significantly differs from other generations of solar cells in the way they operates. They closely mimic the natural photosynthesis carried out by plants. In this process light is absorbed by different substances and charge carries are also different. By means of an electrochemical process, when sunlight is shone on the organic dyes electricity is generated. The first electrode to be employed in DSSCs was coated with ZnO. Through the injection of excited dye molecules into a semiconductor with a large band gap, it was sensitized with chlorophyll, and photons were then converted to electricity [5].

Working principle of DSSCs involves four steps [61], [62]. First, semiconductor photo anode on to which dye molecule are adsorbed absorbs the solar light. In the second step, the absorbed light in turn excites the electrons from the valence band to the conduction band resulting to a flow of the electric current. This current flows through the outside circuit and is gathered by the counter electrode's transparent conductive substrate. Thirdly, the electrolyte solution plays a key role of regenerating the oxidized dye via the redox system in the electrolyte solution and lastly, through a counter electrode the redox system is generated. The operation principle can also be summarized as shown in Figure 5 whereby the following process are involved:

absorbing light, separating charges, and collecting charges [1].
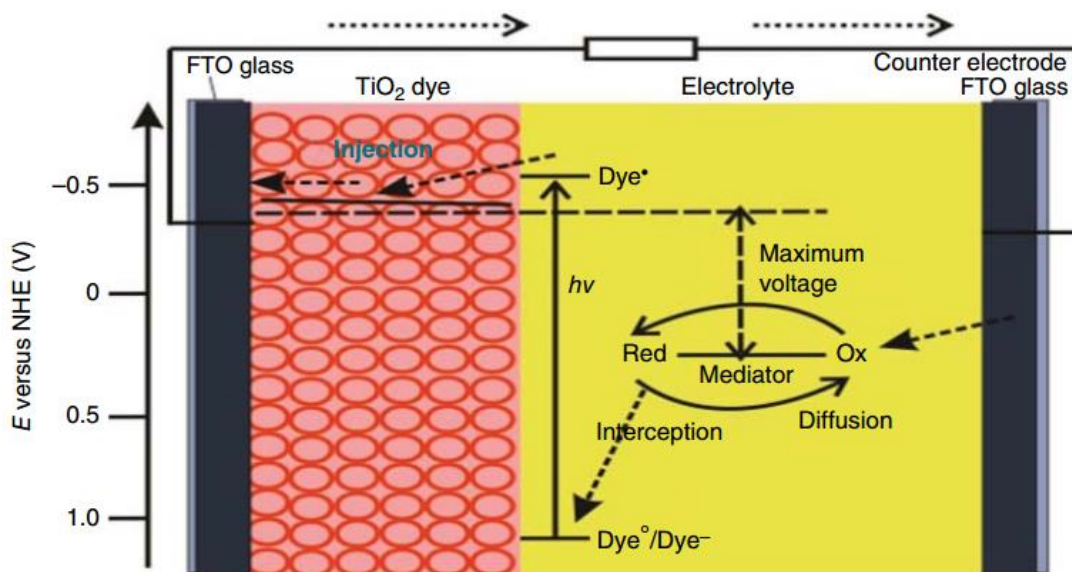
Figure 5 : Schematic diagram of the working principle of DSSCs [1]

The organic hole conductor or the redox electrolyte are in touch with the mesoscopic semiconductor oxide sheet. The dye sensitizer monolayer is adhered to the nanocrystalline film's surface. Under sunlight irradiation, the dye sensitizer absorbs photon and thereafter the absorbed energy excites the electron from highest occupied molecular orbital (HOMO) to lowest unoccupied molecular orbital (LUMO) level of the

dye molecule and become photo excited [63]. In other words, as depicted in Figure 6, the dye's HOMO will release an excited electron, S*, at the LUMO in response to the absorption of light. Charge separation occurs across the dye and TiO_2 interface. Electrons are therefore injected by the adsorbed dye molecules from LUMO level of dye into the conduction band of the mesoporous TiO_2 photoanode.
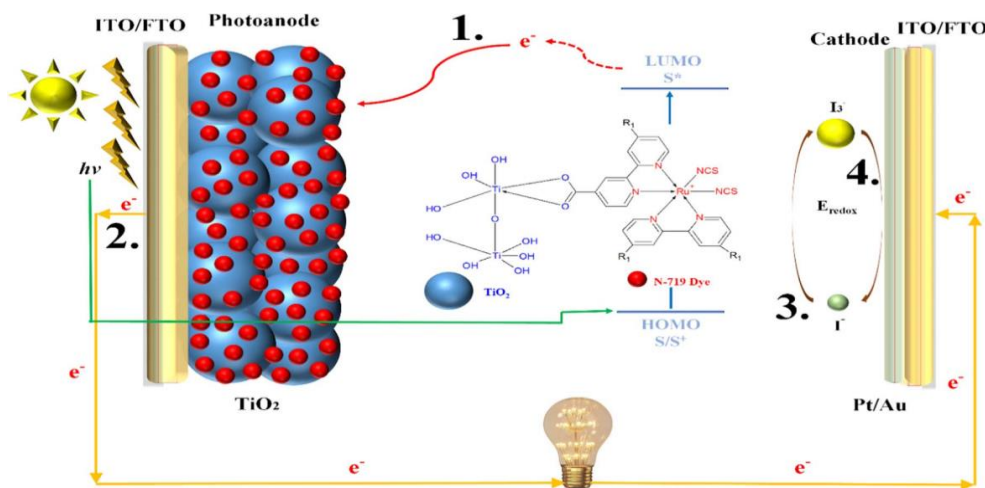
Figure 6: Schematic diagram of the working principal of a dye sensitized solar cell [64].

The S* will subsequently be excited by light and transferred to the photo anode (conduction band), as illustrated in equation 1 [66]. The S* will then transfer an electron, and S^+ will flow via the outer circuit to the cell's cathode, as shown in equation 2 [66]. According to equation 3 [66], the regeneration process is carried out by a redox reaction in which S^+ oxidizes the liquid iodide electrolyte, I-, to produce tri-iodide, I_{3-}, which then neutralizes the state of the sensitizer, S. The electron also lowers the I in equation 4 at this time. This mechanism is shown below

Photo anode:

$$s + hv \rightarrow s^* \qquad\qquad 1$$

$$s^* \rightarrow s^+ + e^-(TiO_2) \qquad\qquad 2$$

$$s^+ + \frac{3}{2}I^- + e^- \rightarrow s + \frac{1}{2}I^{-3} \qquad\qquad 3$$

At the cathode

$$I^{-3} + 2e^-(Pt|Au) \rightarrow 3I^- \qquad\qquad 4$$
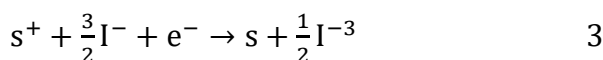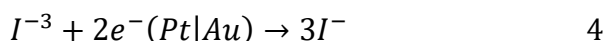
Charge collection occurs when the electrons that were passed through the porous TiO_2 network get to the back contact of the working electrode. Extracted charge returns to the counter electrode, where platinum is deposited on an FTO glass substrate, and also performs electrical work in an external circuit. Oxidized platinum (+2) from the electrolyte receive electron from the external circuit thereby reduced to platinum (0). By donating an electron to the electrolyte once more, platinum is oxidized. Redox process takes place in the iodine electrolyte, which produces the dye molecules. In the electrolyte, the iodine molecule and iodine ion combine to form the triiodide ion. This ion then takes an electron from the counter electrode, reduces, and eventually splits into three iodide ions. Iodide ions are once more converted to triiodide ions by giving electrons to the dye. The oxidized dye is then reduced by the liquid redox electrolyte, which completes the circuit. The difference between the

fermi-level of the electrons in the solid and the electrode's redox potential correlates to the voltage produced during irradiation as seen in Figure 7 [65].
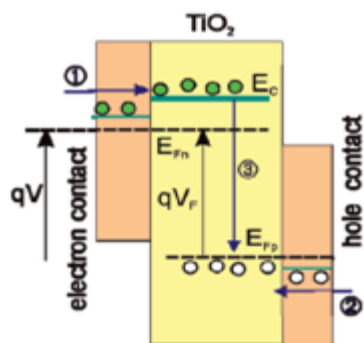
Figure 7: Diagram of voltage injection of electrons and holes in a DSSC recombination process. Additionally displayed are the Fermi levels of electrons and holes, their transport energy levels, the potential V applied between contacts, and the potential VF related to the separation of Fermi levels [67].

The process of electron transfer that takes place in a Ru-complex DSSCs whose photoanode is TiO_2, using an iodide/tri-iodide couple, and a platinum counter electrode, is depicted in Figure 8.

Emphasis on the process of electron transfer and the various energy levels are shown[68]. The DSSCs' electron transport mechanism is depicted in equations 5–10.

$$TiO2/S + Photon\ (h\nu) \rightarrow s * \text{ (Excitation process)} \qquad 5$$

$$TiO_2/S^* + TiO_2 \rightarrow TiO_2/S^+ + e^-_{(CB)} \text{ (Injection process)} \qquad 6$$

$$TiO_2/2S^+ + 3I^- \rightarrow TiO_2/2S + I_3^-\ e^-_{(CE)} \text{ (Regeneration)} \qquad 7$$

$$I_3^- + 2e^- \rightarrow 3I^- \text{ (Reduction)} \qquad 8$$

$$I_3^- + 2e^- \rightarrow 3I^- \text{ (Re} - \text{caption in dark reaction)} \qquad 9$$

$$TiO_2/S^+ + e^-_{(CB)} \rightarrow TiO_2/S \text{ (Recombination in dark reaction)} \qquad 10$$
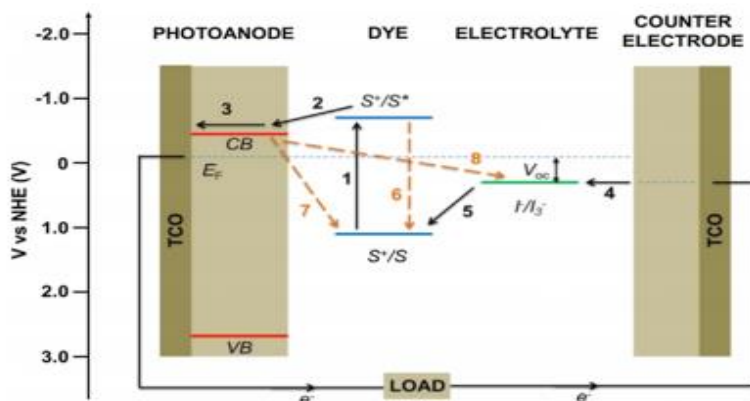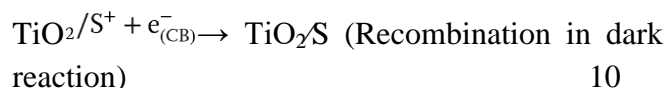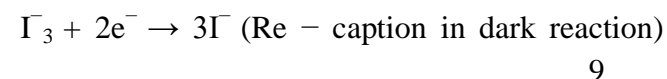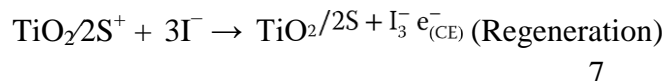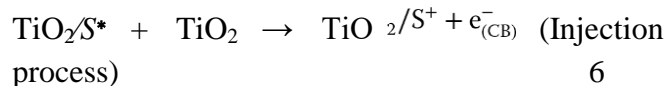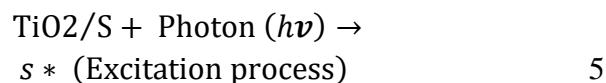
Figure 8: Electron transfer mechanism and energy level diagram of DSSCs [66]

The electron life time τ_n in a DSSC is a central factor in determining the recombination dynamics of a solar cell. It can be determined by V_{oc} decay method. The reciprocal of the open-circuit voltage decline, normalized to the thermal voltage, is used to calculate the lifetime of an electron.

$$\tau_n = -\frac{K_B}{q}\left(\frac{dV_{oc}}{dt}\right)^{-1} \qquad 11$$

Where K_B is the Boltzmann's constant, T is the temperature and q is the elementary charge [65].

Another parameter that sheds light on the recombination characteristics of DSSCs is recombination resistance.

$$R_{rec} = \frac{1}{A}\left(\frac{\partial J_{rec}}{\partial V_{oc}}\right)^{-1} \qquad 12$$

Where J_{rec} is the recombination current and A is the area of the cell.

A good solar cell performance should have shorter carrier extraction time compared to recombination time.
The electron lifetime τ_n compared to the characteristic transport τ_d relates the electron diffusion coefficient, D_n and the active film thickness L as

$$\tau_d = \frac{L^2}{D_n} \qquad 13$$

Diffusion length is another way that can be compared with the film thickness,

$$L_n = \sqrt{D_n \tau_n} \qquad 14$$

Given that the diffusion length, L_n, measures the typical distance that a carrier diffuses before dissipating due to recombination, a high collection efficiency is attained when $L_n > L$ [65]. The inverse relation between the electron lifetime and the steady-state carrier density is a clear indication that the probability of electron recombination depends on the concentration of electrons and holes. There is a direct relationship between the open circuit voltage V_{oc} and the separation distance the Fermi levels of holes and electrons (E_{fp} and E_{fn}) respectively. This relation is given by:-

$$-qV_{oc} = E_{fn} - E_{fp} \qquad 15$$

In DSSC devices V_{oc} is taken to be the upper limit difference in energies between the HOMO and the LUMO. At these high energies, there is no possible split of Fermi density of states and thus, the V_{oc} can be expressed in terms of the band gap energy and the charge present.

$$V_{oc} \approx \frac{E_g}{q} \qquad 16$$

Where
$$E_g = E_{HOMO} - E_{LUMO} \qquad 17$$

This is the effective (electrical) band gap of the dye [67].

The semiconductor's band gap energy plays a pivotal role in the photoelectric conversion of a solar cell. Photo corrosion frequently occurs in semiconductors that use small band gaps to absorb visible light. Other semiconductors, such TiO_2 and Nb_2O_5, show stability under solar illumination and have a large bandgap to efficiently correct visible light. Using visible-light sensitive dye molecules, dye sensitized solar cells address this issue by surface-modifying semiconductors [68].
In an effort to maximize the efficiency of DSSCs, many researchers are seeking new dyes and electrolytes as well as trying to improve on the available electrodes (photo anodes and counter electrodes) [69].

1.5. Components of DSSCs
The ability of a DSSC to convert light photons into electricity involves various processes which includes sensitization of large band gap semiconductors, onto which a light sensitive dye has been adsorbed on the photo-electrode. An appropriate counter electrode and a suitable electrolyte are of consideration for an effective DSSC [51].

1.6. Electrodes used in DSSCs
1.6.1. Conventional Electrodes (Photo Anode and Counter Electrode)
Dye sensitized solar cells uses semiconductor oxides as their electrodes (see
Table **2** and **Error! Reference source not found.** for the conventional electrodes used in natural DSSCs and synthetic DSSCs respectively). The anatase form of TiO_2 is the commonly used semiconductor oxide [70]. Other semiconducting

oxides have also been utilized in DSSC, such as ZnO [71] and SnO$_2$ [72] ,CeO$_2$, CuO, and CdO, although their performance was inferior to that of cells made using TiO2 [73]. The TiO$_2$ is a wide bandgap semiconductor, $E_g \sim 3.2$ eV. The TiO$_2$ has advantages over the other semiconducting counterparts such as not being toxic, cheap, as well as being easily available making it to n be best suited for DSSC applications,. The TiO$_2$ is used as a photoanode in DSSCs applications [68].

Due to its excellent electrical conductivity and stability, platinum (Pt) is frequently utilized for applications.

Materials used for counter electrode applications are desired to poses good electrical conductivity and stability. Platinum (Pt), besides manifesting these qualities, it is also the preferred material for this application due to its favorable electrochemistry with iodide/triiodide redox electrolytes. Another crucial factor to consider in determining a cathode material for DSSC device is the charge transfer resistance (RCT) since it regulates the transfer of electrons between the electrode and the electrolyte [74].

The RCT corresponds to the transfer resistance of electrons at the interface of the counter electrode and the electrolyte. The counter electrode is crucial in that it serves as both a catalyst for the redox couple's regeneration in the electrolyte and the recipient of electrons from the photoanode

The counter electrode plays the important role of collecting electrons from the photoanode and acts as a catalyst for the regeneration of the redox couple in the electrolyte [75]. Counter electrode plays a major role, in that the reduction of mediator takes place there [51]. It enables electron transfer back to the redox electrolyte which comes from the external circuit. It also serves to carry the photo-current over the width of each solar cell.

1.6.2.   Graphene as an Electrode

One of the most promising materials in the field of solar cell technology is graphene, an allotrope of carbon. Carbon atoms with sp^2 hybridization are crammed into a 2D nanostructure to form the transparent layer of graphene, which is only one atom thick. At ambient temperatures, few-layer graphene (FLG) has carrier mobilities of 10,000 cm^2/Vs [76]. Figure 9 shows other related structures which includes fullerene, carbon nanotubes, and graphite.
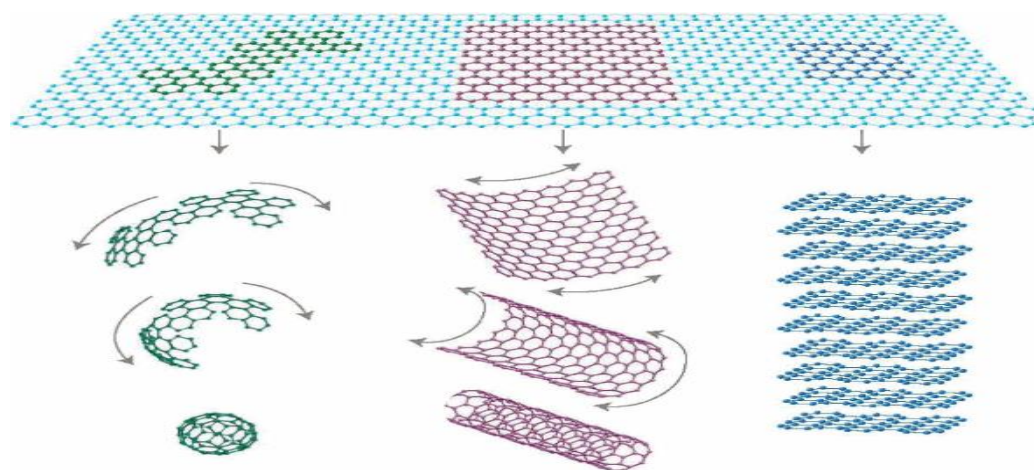
Figure 9: The base of all graphites serves as a 2D building block for all other carbon-based compounds. It can be formed into thick 0D balls, thin 1D nanotubes, or stacked 3D graphite. [77].

Measured optical transparency for a single layer graphene was reported to as 97.7% [78]. This was found to be decreasing as the number of graphene layers were increased. Each additional graphene layer added 2.3% opacity.

Researchers have observed sheet resistance values of 2.1 kΩ/sq for a single layer of graphene and

350 Ω/sq for a four-layer structure with 90% optical transparency at a wavelength of 550 nm [79]. Therefore, as the number of graphene layers rises, the optical transparency and resistance of graphene decrease. Thus, while choosing a material for solar cell applications, high carrier mobility, low sheet resistance, and high optical transparency are crucial considerations. Graphene fulfills this description of a transparent conductive electrode (TCE) material admirably.

Research has shown that graphene is one of the strongest materials with a Young's modulus of 1.02 tera pascals (TPa) [80]. A thermogravimetric analysis (TGA) of graphene oxide (GO) revealed that graphene first undergoes reduction at 100 ^{o}C where absorbed water molecules are extracted, and a subsequent 30% weight loss occurs between 110 and 230 ^{o}C due to the removal of oxygen functional groups from the GO surface [81]. The removal of oxygen functional groups boosts the thermal stability of rGO, which only loses 2% of its weight at 700 ^{o}C in a nitrogen atmosphere, as demonstrated by TGA on rGO[82]. Graphene is suited for application in DSSCs due to the distinct electrical, mechanical, thermal, chemical, and optical properties it possesses as a result of its 2D characteristics. The unique electrical, mechanical, thermal, chemical, and optical qualities that graphene possesses as a result of its 2D features make it suitable for use in DSSCs.

Pure graphene functions as a semimetal since it has no bandgap. In order to make an artificial bandgap in graphene, which is a crucial need for the production of electronic devices, researchers are investigating novel chemical and physical methods that can be employed to open up graphene's band gap. Through hydrogenation by the creation of sp^3 C-H bonds, wide-bandgap semiconductor was created from zero bandgap graphene [83]. Opening up graphene band gap was successfully done by [84], using Ir (111) substrate under controlled hydrogenation. This process significantly changed its physical, chemical, and electrical properties [85].

Dye sensitized solar cells uses titanium dioxide as the photoanode. To enhance the DSSCs' efficiency, changes in the electrodes are inevitable. Graphene has excellent properties such high electron mobility 1500cm^{2}Vs^{-1}, high specific surface area of 2.675m^{2}g^{-1}, as well as being easily dispersed in polymers and solvents, high Young's modulus and being transparent. These properties can be utilized to improve the performance of the DSSCs [75].

Graphene-based materials such as graphene oxide and rGO materials are being explored as new counter electrode materials for DSSCs because of their excellent characteristics which includes electrochemical catalytic activities, high conductivities, high surface areas, corrosion resistance, low weight, and low cost of production. Various factors which affect the photovoltaic performance of DSSCs, includes the materials used for photoanode and counter electrode [75].

Graphene and graphene-based materials plays a crucial role in the photoanode as well as in the counter electrode in as far as the PCEs of DSSCs is concerned.

Table 2 summarizes the photovoltaic performance of DSSCs in terms of short-circuit photocurrent (I_{SC}, open-circuit voltage (V_{OC}), fill factor (FF), and power conversion efficiency (PCE; η).

Photoanode	Counter electrode(CE)	Dye Used	Voc (V)	Isc (mA/cm2)	Vmax(V)	Imax (mA/cm2)	Fill Factor (FF)
TiO2	TiO2-GO	Oliender flowers	0.387	1.539	0.230	1.230	0.47
TiO2	TiO2-rGO	Oliender flowers	0.423	2.411	0.239	2.038	0.47
TiO2	Pt	I. Coccinea	0.316	0.750	0.175	0.567	0.41
TiO2	Pt	I. Coccinea	0.457	1.784	0.265	1.514	0.49
TiO2	TiO2-GO	E.Variegata	0.434	1.394	0.274	1.101	0.49
Graphene-TiO2	Pt	E.Variegata	0.489	1.847	0.279	1.534	0.47
TiO2	rGO	N719	0.669	12.5	-	-	0.660
TiO2	Graphene FTO	N719	0.684	9.475	-	-	0.405
TiO2/rGO	Pt	N719	0.704	8.769	-	-	0.720
TiO2/rGO	Pt	Amaranthus dye	0.3547	1.0042	0.2490	0.5528	0.3864
TiO2	Graphite	Henna dye	0.5478	0.4236	0.3265	0.2737	0.3851
TiO2	Graphite	Roselle dye	0.794	1.2	0.542	0.479	77.93
TiO2	Graphite	N719	0.668	0.95	0.266	0.44	52.62
TiO2	Graphite	Pomegranate	0.39	12.20	0.23	8.5	0.41
TiO2/rGO	FTO painted with colloidal graphite	Black berry	0.47	11.16	0.20	6.98	0.26
TiO2	FTO painted with colloidal graphite	Cranberry	0.41	6.78	0.27	4.31	0.42
Graphene-TiO2	Pt	Blue berry	0.42	2.72	0.25	1.78	0.38
		N719	6.24	10.80	0.31	6.46	0.3
		N719	0.66	6.87	0.37	4.33	0.35
		N719	0.77	3.70	-	-	0.59
		Raspberries	0.429	0.269	-	-	64.8

Shami berries	0.419	0.195	-	-	58.6
Grapes	0.340	0.091	-	-	61.1
Hibiscus flowers	0.388	0.161	-	-	60.0
Combination of dyes	0.4200	0.600	-	-	60.2
Spinach	0.59	0.41	0.46	0.309	58.75982
Red Onion	0.48	0.24	0.34	0.158	46.63194
Red cabbage	0.51	0.21	0.32	0.156	46.61064
Malus domestica (apple)	0.28	2.44	-	-	0.75
Punica granatum(pomegranate)	0.29	3.68	-	-	0.59
Raphanus sativus (red radish)	0.28	2	-	-	0.63
Solunum melongea (egg plant)	0.28	3.85	-	-	0.62
Phoenix dactylifera(date)	0.29	2.45	-	-	0.63
Malus domestica(apple)	0.32	4.48	-	-	0.59
Punica granatum (pomegranate)	0.32	4.5	-	-	0.70
Raphanus sativus (red radish)	0.33	3.12	-	-	0.71
Solunum melongea (egg plant)	0.33	4.51	-	-	0.74
Phoenix dactylifera(date)	0.33	4.21	-	-	0.58
sweet potato leaf	0.65	1.23	-	-	49
Blue berries	0.67	0.532	-	-	61
Purple cabbage	0.64	0.642	-	-	55
Grape	0.71	0.503	-	-	45
Sweet potato and blue berries	0.69	0.42	-	-	28
Sweet potato and purple cabbage	0.645	0.534	-	-	60
Sweet potato and grape	.0675	0.508	-	-	54
Lemon leaves	0.592	1.08	-	-	0.1
Red Bougainvillea	0.492	0.335	-	-	0.25
Orange Bougainvillea	0.465	0.32	-	-	0.06
Morulamorula	0.472	0.059	-	-	0.05

Table 3: Synthetic dyes in DSSCs demonstrates how adding graphene or rGO to the TiO_2 photoanode boosted the power conversion of the manufactured dye-sensitive solar cell. Similarly, when graphene or reduced graphene oxide is used as a counter electrode in place of platinum, the power conversion efficiency of the cell improved. In their study, [73] showed that few layered graphene (FLG)/TiO_2 nanocomposites exhibited superior photovoltaic properties Compared to TiO_2 nanoparticles (NPs) and other FLG/MO (CeO_2, CuO, SnO_2, CdO, ZnO,) nanocomposites. Reference [86], incorporated graphene in TiO_2 photoanode with various weight ratios of graphene. According to their findings, three layers of nanocomposites coated on electrodes outperformed one or two layers of graphene and sped up electron transit. It was showed that 0.005 was the best suitable graphene ratio, increasing efficiency by 22% above that of the conventional DSSC. [146]

For charge transport in DSSCs, which use redox mediators, the reduced species regenerates the dye while the oxidized species is reduced at the cathode. Redox species reduction rate must be slow at the anode and rapid at the cathode, dye regeneration from reduced species must occur more quickly than from the semi-conducting scaffold, and these requirements must all be met for the system to work properly. A material that is more catalytic is desirable at the cathode to lower the excess voltage needed to reduce the mediator species. Due to their simple manufacture and high activity, notably for the iodide/triiodide mediator, FTO's coated with platinum have extensively been used as cathodes [87].

Few layers of graphene (FLG) were introduced into the counter electrode (CE) in [88]. According their findings, the placement and the number of graphene layers in the CEs had a significant impact on how well DSSCs converted energy and reduced the need for Pt. The CEs in two graphene regions were investigated: (1) The interface between Pt and fluorine doped tin oxide (FTO) to improve contact at the Pt/FTO junction, and (2) the interface between Pt and electrolyte to enhance the device's electrocatalytic capabilities. Figure 10 illustrates the CEs with the various graphene and Pt layer sequences that were employed, including (1) Pt over graphene (Pt/graphene) and (2) graphene over Pt (graphene/Pt). They discovered 8% improvements in short-circuit current density (Jsc) and 12.5% improvements in power conversion efficiency (PCE) for Pt/FLG devices, while a 21% reduction in contact resistance was achieved when FLG was used at the point where Pt and FTO meet.
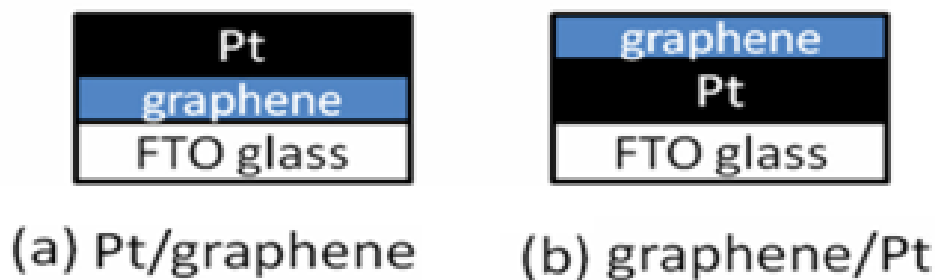
Figure 10: Two different ways of incorporating graphene in a CEs: (a) the Pt/graphene CEs and (b) the graphene/Pt CEs [88].

1.7. Photosensitizers (Dye)

Solar energy harvesting in a DSSC is performed by the photosensitizing dye. Sensitizers play a very important role of absorbing the solar photons besides injecting the photo excited electrons into the conduction band of the n-type material [89]. In order to operate effectively in a DSSC, dye sensitizers must meet a number of criteria, including having a broad absorption spectrum because the maximum photon absorption ranges from the visible to the near infrared region, the capacity to generate photo-excited electrons, and effective charge infusion into the semiconductor layer's conduction band [90].

A suitable sensitizer should have both the carboxyl and hydroxyl groups necessary for strong interaction with the mesoporous semiconductor, should have maximal absorbance within the visible range to the near infrared region of solar radiations, and should not degrade quickly [91]. Photosensitizers that have been explored for DSSC applications include the metal complex sensitizers which have been found to have limitations such as use of rare metals that are costly and are unfriendly to the environment. Other metal free organic sensitizers that have been used was reported to have low power conversion efficiency and the process of synthesis for the sensitizers is complicated. Other available sensitizers are the natural dyes that are environmental friendly and easily biodegradable. Natural dyes can be readily obtained and extracted from the fruits, flowers, leaves, and roots of a variety of plants. [92]

The functional groups in a dye determines its molecular structure for DSSC applications. Excellent adhesion between the TiO_2 semiconductor surface is well achieved when the dye is acidic nature than when it is alkaline ([93], [94]. To ensure that electrons are effectively injected from the dye to the conduction band of the semiconductor, the dye should have a higher energy in comparison to the n-type semiconductor. Other requirements include that the photosensitizers have good photo-stability and that their HOMO should be below the energy level of the redox mediator in order to enhance dye regeneration [97],[98]. Synthetic photosensitizers as well as natural dyes have been studied for applications in DSSCs.

1.7.1. Synthetic Dyes

Many synthetic sensitizers have been developed based on the ruthenium element for use in DSSCs. These ruthenium complexes include N3 ('red' dye), N749 ('black' dye), N719 and Z907 complexes [96]. The dye sensitized solar cells developed by [48] used ruthenium (II)-bipyridyl complex as the sensitizer. This dye demonstrated high stability and light-to-electric energy conversion efficiencies of up to 7.9% [75]. In [97], developed several other ruthenium (II) complexes also known as N3 dye that proved to be the most interesting photo sensitizers absorbing up to 800 nm with a Power conversion efficiency of up to 10% with Lithium Iodide/triiodide as a redox couple [98]. Other ruthenium complexes surrounded by bidentate ligands have also been

developed and used as photoactive dyes. **Error! Reference source not found.** gives a summary of various synthetic dyes that have been developed and used DSSC applications with their highest attained efficiencies. For example, preparation and characterization of ruthenium complexes (5-8A) with different backbone structure for DSSC application yielded power conversion efficiency (PCE) of 0.64-2.25 % [99].

Due to their strong charge-transfer absorption across the whole visible spectrum and effective metal-to-ligand charge transfer, ruthenium dyes have been utilized as efficient sensitizers. Besides possessing these qualities, they have a number of limitations, including a difficult synthesis process, pose a significant threat to life and the environment due to their presence of heavy metals that are deemed carcinogenic, and are not cost-effective [100].

Organic solvents have also been employed as an alternative sensitizer but they have their challenges as well such as being explosive hence it's an environmental hazard. Materials used to fabricate DSSCs that imitate photosynthesis in actual leaves are not friendly to the environment. The process of synthesizing the complex compounds is not only complicatedbut also costly. Other commercial dyes and natural dyes can as well be used as an alternative. Although they are inexpensive and simple to prepare, natural and/or synthetic organic dyes like cyanine dyes, xanthene dyes, and coumarin dyes perform poorly in DSSCs due to their weak binding energy with TiO_2 layer and low charge-transfer absorption throughout the whole visible range [101].

Natural dyes have various merits over the synthetic dyes since they are available in abundance, their extraction process requires minimal chemical procedures, they have large absorption coefficient, they have low cost and are easily biodegradable [102]. Researchers are therefore leveraging on natural dyes as an alternative sensitizer since they can be used can be employed with adequate efficiency for the same purpose.

1.7.2. Natural Dyes

Regarding dye-sensitized solar cells, natural dyes are being looked at as promising photosensitizers due to their low cost, resource reproducibility, non-toxic environmental impact, and wide distribution. Because of their low cost, resource repeatability, non-toxic environmental impact, and widespread use, natural dyes are viewed as viable photosensitizers in DSSCs. The primary benefit of natural-based dyes is that, even with heavy usage, they are never in danger of going extinct. Some plants' flowers, leaves, and fruits can be simply utilized to extract the pigments that make up natural dyes (see

Table **2** for a list of plants from which natural dyes can be produced). Each component of a natural plant has a distinctive pigment hue. Natural dyes that are commonly used in DSSCs have natural compounds such as chlorophyl, anthocyanin, beta-carotene, flavonoids and carotenoid [51], [103]. The absorption range of natural sensitizers is 400–700 nm (visible region range) [104].

1.7.2.1. Flavonoids

The word flavonoid defines a large group of natural product including C_6-C_3-C_6 carbon structure or specifically phenylbenzopyran [51]. Flavone is made up of two benzene rings connected by γ a ring that sets one flavonoid chemical apart from another. Only a few flavonoids can effectively absorb light in the visible spectrum. [105]. Figure 11 is the chemical composition of a flavonoid
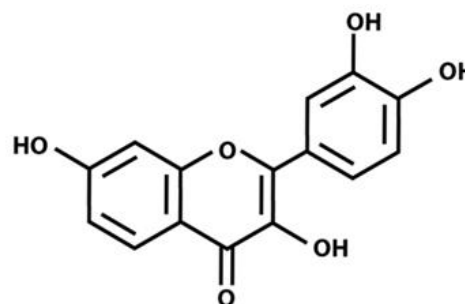
Figure 11: Chemical structure of a flavonoid [106]

Thousands of naturally occurring flavonoids that have successfully been distinguished from plant

extracts and classified as flavonols, flavones, flavanones, isoflavones, catechins, anthocyanin, and chalcones based on their chemical composition [107]. Flavonoids mainly occurs in fruits as well as in flowers where insect pollinators are attracted [51]. Flavonoids' charge transfer, which requires less energy for the shift from HOMO to LUMO, energizes the pigment molecules when exposed to light, creating a broad absorption band in the visible spectrum. [108]. A proton is given by the flavonoid when it quickly adsorbes at the surface of TiO_2, displacing an OH- counter ion from the Ti (IV) site. The flavonoid group's anthocyanins are what give most flowers, fruits, and leaves their various colors, which range from pink to red and violet to dark blue [93].

Studies have shown that flavonoids are useful in DSSCs by the adsorption of flavonoids on TiO_2 nanoparticles or commercial TiO_2 electrodes leading to the development a broad absorption band extending to about 550 nm [109].

1.7.2.2. Carotenoids

They are pigments that are extracted from chloroplast and chloromoplast of plant as well as in photosynthetic organism [110].. [108]. It has a backbone made of C_{40} hydrocarbons, which causes structural and oxygenic alteration as depicted in Figure 12
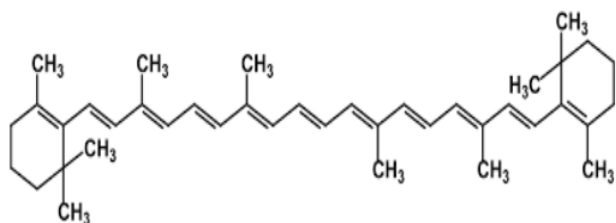
Figure 12 : Structure of Carotenoid [110])

Depending on their chemical structure, carotenoids can be categorized in to two [106].The first structure of carotenoids contain carbon and hydrogen in their structure whereas the second structure contains carbon, hydrogen and oxygen. Additionally, they can be divided into primary and secondary groups. While secondary carotenoids

are concentrated in fruits and flowers, primary carotenoids are essential for plants' ability to perform photosynthesis. Light with a wavelength between 400 and 550 nm is absorbed by all carotenoids.

Studies that report the use of Carontenoids in DSSCs includes [111]–[115], [115]–[117] among others. These studies conclude that due to the anthocyanin dye aggregation on the TiO_2 surface, Anthocyanin-based DSSC should have higher efficiency and a longer lifetime.

1.7.2.1. Anthocyanin

The anthocyanin group is actively researched as a natural sensitizer, and its extracts exhibit maximal absorption between 510 and 548 nm, depending on the fruit or solvent utilized. [118]. Anthocyanin belong to the flavonoid class of natural pigments that are responsible for various color pigments which includes the shiny orange, red, pink, violet and blue colors found in flowers and fruits.

Anthocyanin content and composition in plants are influenced by both hereditary and ecological factors. The basic structures of the anthocyanins are called anthocyanidins (agylycons), and they consist of an aromatic ring (A) attached to a heterocyclic ring (C) that has oxygen, as seen in Figure 13 [119].
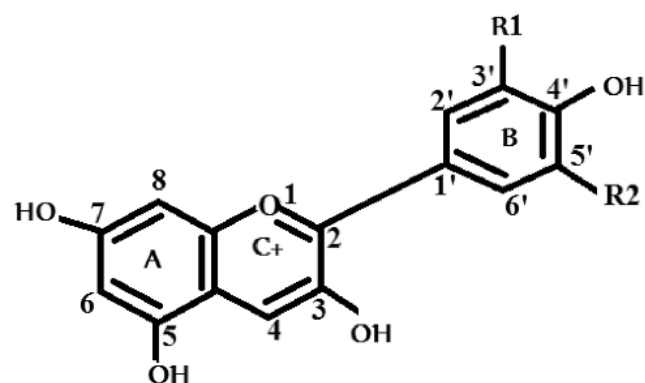
Figure 13: An aromatic hydrocarbon (A), an aromatic hydrocarbon (B), and a heterocyclic ring (C+) that make up anthocyanin's basic structural components [119]

Based on a C15 backbone, anthocyanins are essentially chemically substituted salts of phenyl-

2-benzopyrilium [3]. Figure 14 illustrates its atomic structure.
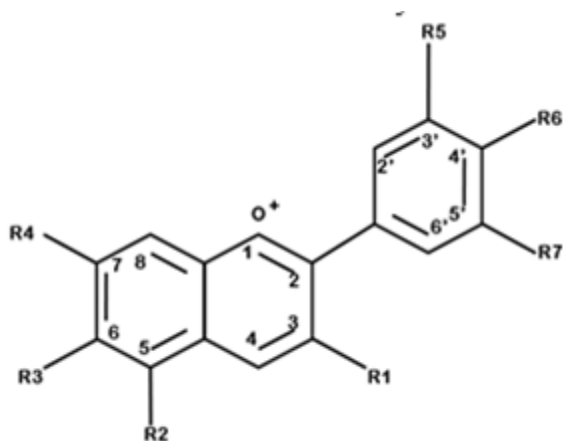
Figure 14: Anthocyanin chemical structure: R could be replaced with either H, OH or OCH3 [106]

There are 17 known anthocyanin structures which are classified depending on the number of sugar molecules which form compound such as monosides, biosides among others [120]. Attractive colors in flowers, fruits, leaves as well as in mosses and fern are due to anthocyanin. Another role played by anthocyanin is modifying the quality and quantity of light incident on the chloroplast [121]. The anthocyanin molecule attached to the TiO_2 semiconductor surface has both carbonyl and hydroxyl groups. This helps to excite and transmit electrons from the anthocyanin molecule to the porous TiO_2 film's conduction band. [108].

Raspberries, Shami berries, grapes, hibiscus, chlorophyll, and a dye mixture were all studied in relation to various anthocyanin-containing natural colors [93]. Using the Sol-Gel process, thin film components FTO/TiO_2/Natural Dye/Electrolyte/ Pt/FTO were prepared, and the performances of various natural dye kinds were evaluated. In comparison to other single dyes, they found that DSSC made using a combination of natural dyes (raspberries, hibiscus, and chlorophyll) in the ratio (1:1:1) had greater photovoltaic performance. The prepared DSSC had an efficiency of = 3.04%, a fill factor of 60%, a cell area of 4 cm^2, a short circuit current of 0.6 mAcm^{-2}, and an open circuit voltage of 0.42 volts.

Other studies that have shown the performance of Anthocyanin in DSSCs include[119], [119], [122], [123]. Overall, it has been demonstrated that using a single anthocyanin results in lower efficiency; as a result, several improvements have been made, including the use of copigmentation and dye mixture [122], extending the working electrode's time in the dye solution [124], and lowering the pH of the dye liquid [125]. These techniques successfully raise the DSSC's efficiency. Anthocyanin dye is a potential alternative to synthetic dye based on the ruthenium complex since it is readily available in nature, simple to produce, and non-toxic.

1.7.2.2. Chlorophyll

It is a substance that is also known as a chelate and is made up of a big organic molecule attached to a central metal ion in addition to hydrogen and carbon [110]. In order for carbon dioxide to be converted into carbohydrates and water to be converted into oxygen during photosynthesis, it must first absorb the energy necessary for these reactions. Chlorophyll has two types, a and b, as depicted in Figure 15.
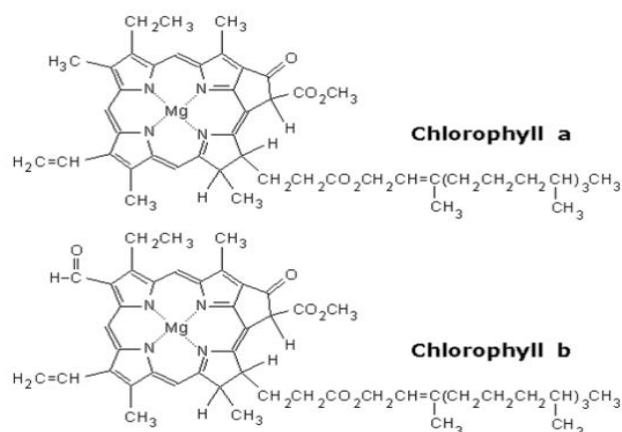
Figure 15: Chemical structure of two types of chlorophyll a and b [110]

Due to their beneficial light absorption tendancy, derivatives of chlorophyll are utilized in DSSCs as dye sensitizers [126]. As an efficient compound, chlorophyll acts as photosensitizer in the visible

light and have a maximum absorption at wavelength of 670 nm. Chlorophyll-a with composition $C_{55}H_{72}O_5N_4Mg$ which is responsible for photosynthesis in plants has absorption peaks at 430nm and 662 nm. The absorption peaks of chlorophyll-b, which has the chemical formula $C_{55}H_{70}O_6N_4Mg$ are at 453 nm and 642 nm.
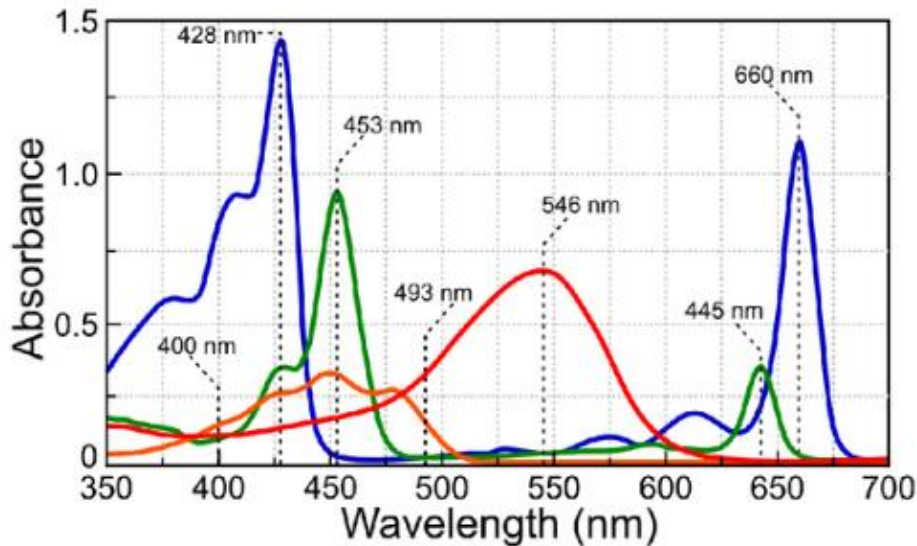
Figure 16: Chlorophyll a (blue), Chlorophyll b (green), -carotene (orange), and anthocyanin (red) absorption spectra of freshly isolated pigments [127].

According to studies, mixing the aforementioned dyes frequently leads to higher photoconversion efficiencies since there are more functional groups available to connect the dye to the TiO2 semiconductor surface. This increases dye adsorption and coverage and leads to the formation of an efficient organic passivation layer that inhibits back carrier recombination [128] enhanced visible-light photo-electrochemical performance and light stability [129] among others. Other research, such as that in [130], which combined five different plant extracts from *Amaranthus caudatus, Bougainvillea spectabilis, Delonix regia, Nerium oleander,* and *Spathodea companulata*, has revealed that combined plant extracts don't always exhibit synergistic photosensitization in comparison to the separate extracts.

In the past, most of the plants that have been researched on as the sources of natural sensitizers such as the flavonoids, carotenoids, anthocyanins, and chlorophyll are food related as shown in Table **2** and hence exert pressure to the energy-food-water nexus. These plant as shown in Tabke 2 include Shami berries, Grapes, Hibiscus flowers, Spinach, Red Onion, Red cabbage and Malus domestica (apple). Alternative plants such as the weeds that are easily available, ecofriendly and don't exert pressure to energy-food-water nexus such as *Tithonia diversifolia*, *Tagetes minuta* and *Bidens pilosa* are an alternative source that is expolorable (see Figure 17)
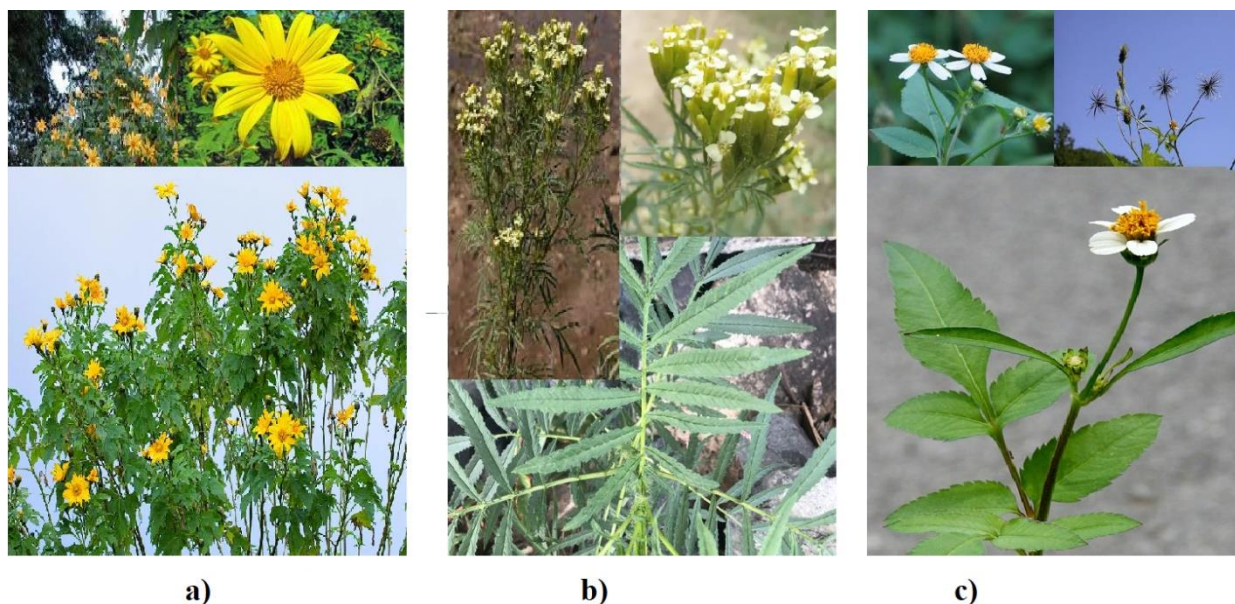
Figure 17: Naturally occuring weeds a) Tithonia diversifolia, b) Tagetes minuta and c) Bidens pilosa

1.7.2.3. *Tithonia diversifolia* (Mexican Sunflower/ Tree Marigold)

The *T.diversifolia* is a common shrub that is commonly used on field boundaries and glass lands. It is an invasive weed that often grows in tropical ecosystems and is well-suited to a variety of situations. It has the benefit of being able to occupy diverse degraded regions due to its ability to adapt to different environmental circumstances (climate and soil), and it quickly outcompetes local species. [131].

Sesquiterpene lactones, flavonoids, and trans-cinnamic acid are some of *T. diversifolia's* chemically active components. The flavonoids are of great use as sensitizers in the DSSCs due to the presence of the hydroxyl and carboxyl groups. The UV spectrum of the flavonoids has two peaks with band 1 ranging at 300-400 nm while band 2 ranges at 240-280 nm [132].

1.7.2.4. *Tagetes minuta* (Mexican Marigold)

Tagetes minuta (Mexican marigold) is an invasive weed that grows well in disturbed areas and cultivated beds. It contains active chemical ingredients such as acyclic monoterpene, sesquiterpene, flavonoids, thiopenes, chlorophyl

and carotenoids [133]. The flavonoids, carotenoids and chlorophyl are of great use as photosensitizers in Dye sensitized solar cells. The UV-Vis spectrum of the dyes ranges between 280 to 360 nm [134].

1.7.2.5. Bidens Pilosa (Black Jack)

Bidens pilosa (black jack) is a perennial herb that is globally distributed across the temperate and tropical regions. Its major chemical ingredients include polyacetylenes, flavonoids and triterpenes. Flavonoids and phenolics as well as their derivatives are usually found on the leaves stems and roots of the plant [135]. The UV-Vis Spectrum of dyes ranges between 200 nm to 400 nm [136]. The roots reveal a higher absorption spectrum compared to the stem while the leaves have the lowest absorption spectrum [137].

1.8. Solar Cell Performance Parameters

Various cell metrics such as the open circuit voltage (V_{oc}), short circuit current (I_{sc}), fill factor (FF), maximum voltage (V_{max}), and maximum current (I_{max}), are used to assess the performance of dye sensitized solar cells (DSSCs) [91]. See Table **2** and **Error! Reference source not found.** for some of the parameters determined in both natural and synthetic DSSCs)

1.8.1. Open circuit voltage

At the solar cell's open terminals, the open circuit voltage (V_{oc}) is specified. The V_{oc} drops as the cell's temperature rises. Equation 18 represents the cell's Voc.

$$V_{OC} = V_t \ln \left\{ \left(\frac{I_{sc}}{I_o} \right) + 1 \right\} \qquad 18$$

V_t is the terminal voltage of the cell [91].

1.8.2. Short circuit current

The short circuit terminals of the cell are used to compute the short circuit current (I_{SC}). As temperature rises, the short circuit current increases as well [138].

The I_{sc} is expressed:

$$I_{sc} = I + I_o \left(\exp \left(V/V_t \right) - 1 \right. \qquad 19$$

1.8.3. Fill factor

The ratio of the actual power (the product of the maximum voltage, V_{max}, and the maximum current, I_{max}) to the dummy power (the product of V_{oc} and I_{sc}) is known as the fill factor (FF) of the solar cell [139].

$$FF = \frac{V_{max} I_{max}}{V_{oc} I_{sc}} \qquad 20$$

1.8.4. Efficiency

The ratio of electrical power to optical power incident on the cell is used to define the efficiency of the solar cell. It is written as follows:

$$\eta = FF. Voc. Isc/\text{Incident optical power} \qquad 21$$

where;

η is the solar cell efficiency [91].
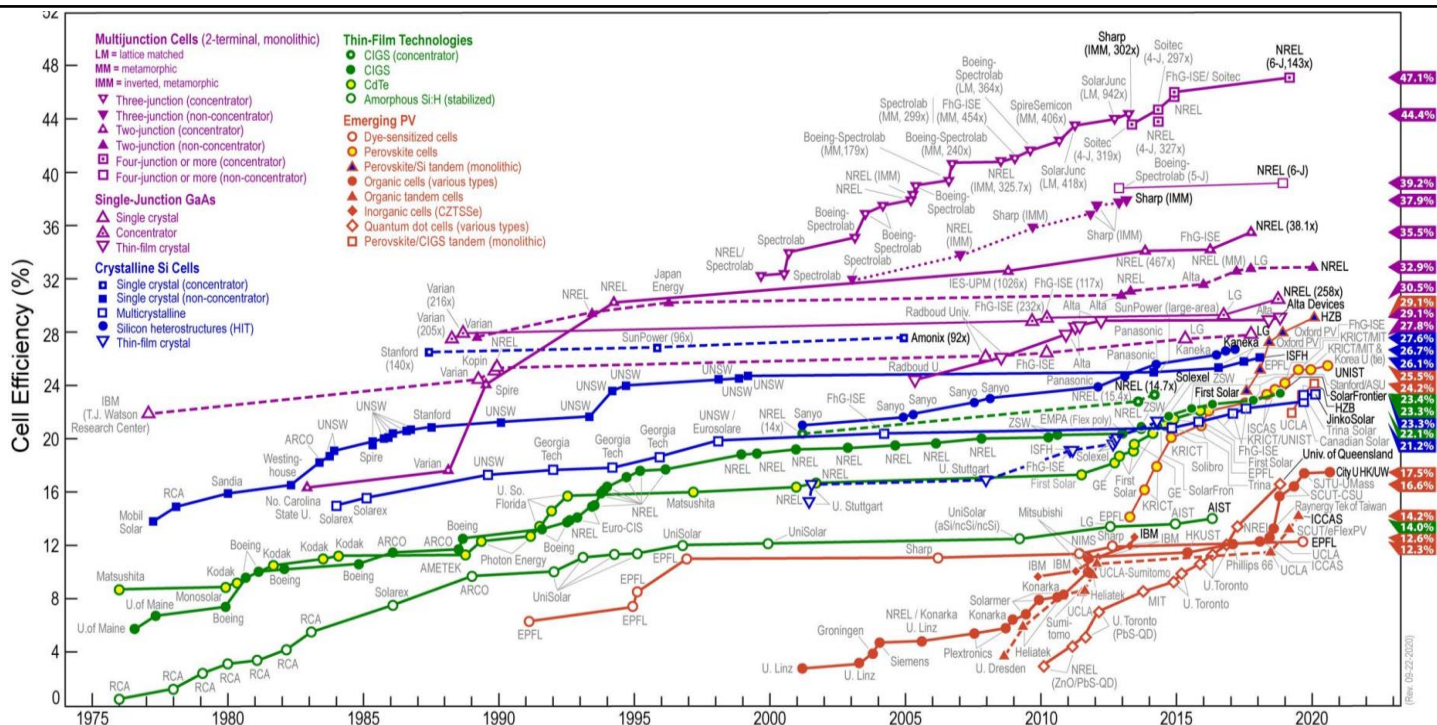
Figure 18: Best Research cell efficiencies (NREL 2020)

Table 2: A comparison of various natural and ruthenium dyes in DSSCs applications

Photo anode	Counter electrode(CE)	Dye Used	V_{oc} (V)	I_{sc} (mA/cm^2)	V_{max}(V)	I_{max} (mA/cm^2)	Fill Factor (FF)	Efficiency(η)	Reference
TiO$_2$	Pt	Oliender flowers	0.387	1.539	0.230	1.230	0.47	0.33	[140]
TiO$_2$-rGO	Pt	Oliender flowers	0.423	2.411	0.239	2.038	0.47	0.57	
TiO$_2$	Pt	I. Coccinea	0.316	0.750	0.175	0.567	0.41	0.11	
TiO$_2$-rGO	Pt	I. Coccinea	0.457	1.784	0.265	1.514	0.49	0.47	
TiO2	Pt	E.Variegata	0.434	1.394	0.274	1.101	0.49	0.35	
TiO$_2$-rGO	Pt	E.Variegata	0.489	1.847	0.279	1.534	0.47	0.50	
Graphene-TiO$_2$	Pt	N719	0.669	12.5	-	-	0.660	5.52	
TiO$_2$	rGO	N719	0.684	9.475	-	-	0.405	2.622	[141]
TiO$_2$	Pt	N719	0.704	8.769	-	-	0.720	4.446	
TiO$_2$	Graphene FTO	Amaranthus dye	0.3547	1.0042	0.2490	0.5528	0.3864	0.14	[142]
TiO$_2$	Graphene FTO	Henna dye	0.5478	0.4236	0.3265	0.2737	0.3851	0.09	
TiO$_2$/rGO	Pt	Roselle dye	0.794	1.2	0.542	0.479	77.93	0.743	[143]
TiO$_2$/rGO	Pt	N719	0.668	0.95	0.266	0.44	52.62	0.334	
TiO$_2$	Graphite	Pomegranate	0.39	12.20	0.23	8.5	0.41	2.0	[144]
TiO$_2$	Graphite	Black berry	0.47	11.16	0.20	6.98	0.26	1.4	
TiO$_2$	Graphite	Cranberry	0.41	6.78	0.27	4.31	0.42	1.2	
TiO$_2$	Graphite	Blue berry	0.42	2.72	0.25	1.78	0.38	0.4	
TiO2/rGO	FTO painted with colloidal graphite	N719	6.24	10.80	0.31	6.46	0.3	2.02	[145]
TiO2	FTO painted with colloidal graphite	N719	0.66	6.87	0.37	4.33	0.35	1.61	
Graphene-TiO$_2$	Pt	N719	0.77	3.70	-	-	0.59	2.56	[86]
TiO$_2$	Pt	Raspberries	0.429	0.269	-	-	64.8	1.50	[93]
TiO$_2$	Pt	Shami berries	0.419	0.195	-	-	58.6	1.50	
TiO$_2$	Pt	Grapes	0.340	0.091	-	-	61.1	0.38	
TiO$_2$	Pt	Hibiscus flowers	0.388	0.161	-	-	60.0	0.75	
TiO$_2$	Pt	Combination of dyes	0.4200	0.600	-	-	60.2	3.04	
TiO$_2$	Pt	Spinach	0.59	0.41	0.46	0.309	58.75982	0.171253	[146]
TiO$_2$	Pt	Red Onion	0.48	0.24	0.34	0.158	46.63194	0.064723	
TiO$_2$	Pt	Red cabbage	0.51	0.21	0.32	0.156	46.61064	0.060145	
ZnO	Graphite	Malus domestica (apple)	0.28	2.44	-	-	0.75	0.51	[147]
ZnO	Graphite	Punica granatum(pomegranate)	0.29	3.68	-	-	0.59	0.63	
ZnO	Graphite	Raphanus sativus (red radish)	0.28	2	-	-	0.63	0.35	
ZnO	Graphite	Solunum melongea (egg plant)	0.28	3.85	-	-	0.62	0.67	
ZnO	Graphite	Phoenix dactylifera(date)	0.29	2.45	-	-	0.63	0.45	
TiO$_2$	Graphite	Malus domestica(apple)	0.32	4.48	-	-	0.59	0.85	
TiO$_2$	Graphite	Punica granatum (pomegranate)	0.32	4.5	-	-	0.70	1.008	

TiO$_2$	Graphite	Raphanus sativus (red radish)	0.33	3.12	-	-	0.71	0.73	
TiO$_2$	Graphite	Solunum melongea (egg plant)	0.33	4.51	-	-	0.74	1.10	
TiO$_2$	Graphite	Phoenix dactylifera(date)	0.33	4.21	-	-	0.58	0.81	
TiO$_2$	Pt	sweet potato leaf	0.65	1.23	-	-	49	0.391	[148]
TiO$_2$	Pt	Blue berries	0.67	0.532	-	-	61	0.218	
TiO$_2$	Pt	Purple cabbage	0.64	0.642	-	-	55	0.226	
TiO$_2$	Pt	Grape	0.71	0.503	-	-	45	0.16	
TiO$_2$	Pt	Sweet potato and blue berries	0.69	0.42	-	-	28	0.08	
TiO$_2$	Pt	Sweet potato and purple cabbage	0.645	0.534	-	-	60	0.207	
TiO$_2$	Pt	Sweet potato and grape	.0675	0.508	-	-	54	0.185	
TiO$_2$	Carbon	Lemon leaves	0.592	1.08	-	-	0.1	0.036	[149]
TiO$_2$	Carbon	Red Bougainvillea	0.492	0.335	-	-	0.25	0.023	
TiO$_2$	Carbon	Orange Bougainvillea	0.465	0.32	-	-	0.06	0.005	
TiO$_2$	Carbon	Morulamorula	0.472	0.059	-	-	0.05	0.0008	

Table 3: Synthetic dyes in DSSCs

Photo anode	Counter electrode(CE)	Dye Used	V_{oc} (V)	I_{sc} (mA/cm^2)	V_{max}(V)	I_{max} (mA/cm^2)	Fill Factor (FF)	H	Refference
TiO$_2$	Pt on FTO glass	Z907	731	13.9	-	-	0.69	7.0	[150]
TiO$_2$	Pt on FTO glass	K51	730	14.8	-	-	0.72	7.2	
TiO$_2$	Pt on FTO glass	K68	762	14.4	-	-	0.69		
TiO$_2$	-	MXD10	635	15	-	-	0.68	6.47	
TiO$_2$	-	YS-1	0.66	13.01	-	-	0.69	5.94	
TiO$_2$	-	YS-2	0.69	14.08	-	-	0.63	6.44	[151]
TiO$_2$	-	YS-3	0.70	15.90	-	-	0.62	6.91	
TiO$_2$	-	YS-4	0.68	14.72	-	-	0.66	6.63	
TiO$_2$	-	YS-5	0.64	15.40	-	-	0.66	6.60	
TiO$_2$	-	Z907	0.68	14.16	-	-	0.66	6.36	
TiO$_2$	-	N719	0.71	15.17	-	-	0.66	7.13	
TiO$_2$	FTO substrate	OD1	0.62	1.82	-	-	71	0.8	[152]
TiO$_2$	FTO substrate	OD2	0.64	3.88	-	-	71	1.76	
TiO$_2$	FTO substrate	OD3	0.58	6.87	-	-	68	2.72	
TiO$_2$	FTO substrate	N719	0.68	17.48	-	-	74.7	8.89	
TiO$_2$	FTO substrate	5T	0.62	17.15	-	-	72	7.64	
TiO$_2$	FTO substrate	6T	0.67	16.85	-	-	62.8	7.07	
TiO$_2$	FTO substrate	Y-1	0.5352	0.4865	-	-	73.19	0.191	
TiO$_2$	FTO substrate	Y-2	0.5281	0.4558	-	-	72.95	0.176	
TiO$_2$	FTO substrate	Y-3	0.5319	0.4344	-	-	73.06	0.169	
TiO$_2$	FTO substrate	S-1	0.5132	0.2974	-	-	73.26	0.113	
TiO$_2$	FTO substrate	S-2	0.5132	0.3508	-	-	73.25	0.131	
TiO$_2$	FTO substrate	S-3	0.5172	0.3247	-	-	73.39	0.123	
TiO$_2$	FTO substrate	B-1	0.4645	0.2221	-	-	66.09	0.068	
TiO$_2$	FTO substrate	B-2	0.4666	0.2089	-	-	65.78	0.064	
TiO$_2$	FTO substrate	B-3	0.4694	0.2011	-	-	65.29	0.062	
TiO$_2$	FTO substrate								
TiO$_2$ nanoparticles	-	SM 315	0.91	18.1	-	-	0.78	13	[153, p. 13]
ZnO	FTO substrate	/7/PF$_6$	0.503	1.68	-	-	48.3	0.4	
ZnO	FTO substrate	/8/PF$_6$	0.492	2.7	-	-	60	0.8	
ZnO	FTO substrate	D149	0.668	8.383	-	-	35	2	
TiO$_2$	FTO substrate	14A-25D	0.5285	4.8	-	0.412	59.35	1.5	
TiO$_2$	FTO substrate	12A-45D	0.648	10.8	-	0.418	63.64	4.5	[154]
TiO$_2$	FTO substrate	N3	0.7258	14.8	-	0.466	69.97	7.5	
TiO$_2$	FTO substrate	XS10	0.621	6.2	-	-	0.67	2.6	[155]
TiO$_2$	FTO substrate	XS10^b	0.611	4.5	-	-	0.68	1.9	
TiO$_2$	FTO substrate	XS11	0.640	7.6	-	-	0.64	3.1	
TiO$_2$	FTO substrate	XS12	0.615	7.4	-	-	0.66	3.0	
TiO$_2$	FTO substrate	XS13	0.642	9.8	-	-	0.63	4.0	
TiO$_2$	FTO substrate	N719	0.714	14.8	-	-	0.63	6.4	
TiO$_2$	-	RD-I	0.742	9.31	-	-	0.72	5	[156]
TiO$_2$	-	RD-II	0.746	13.94	-	-	0.68	7.11	
TiO$_2$	-	CA-I	0.789	8.23	-	-	0.72	4.69	
TiO$_2$	-	CA-II	0.804	11.34	-	-	0.70	6.39	
Al$_2$O$_3$	FTO substrate	Np-TiO$_2$-perylene dye/polymer	0.54	4.37	-	-	0.49	1.15	[157]
Al$_2$O$_3$	FTO substrate	Np-TiO$_2$-perylene dye/polymer	0.61	6.45	-	-	0.54	2.13	
Al$_2$O$_3$	FTO substrate	Np-TiO$_2$-perylene dye/polymer	0.65	8.92	-	-	0.59	3.42	

1.9. Conclusion

In this review paper various generations solar cells have been discussed, the Shockley-Quisser limit that limits the maximum achievable efficiency of solar cells has been well discussed with an emphasis to DSSCs. The working electrode, counter electrode, and numerous dye sensitizers utilized in DSSCs—both synthetic and natural dyes—have all been explored in relation to the structure and operation of DSSCs. A detailed discussion on the DSSC electrodes (the photoanode and the counter electrode) together with the limitations and various modifications that can be made to improve the cell efficiency has been discussed. These modifications, which utilize carbon-based materials like graphene and reduced graphene oxide in the electrodes, have been studied. Various plant pigments employed as sensitizers in DSSCs have been examined in detail and tabulated. Detailed summary of synthetic dye based DSSCs carried out by different groups, have also been reviewed. Finally, the performance parameters of DSSCs have been discussed. Consequently, it is recommended to maximize the usage of DSSCs as a substitute source of energy

1.10. Acknowledgement

1.11. References

1. S. Karthick, K. Hemalatha, S. K. Balasingam, F. Manik Clinton, S. Akshaya, and H. Kim, 'Dye-sensitized solar cells: history, components, configuration, and working principle', *Interfacial Eng. Funct. Mater. Dye. Sol. Cells*, pp. 1–16, 2019.

2. A. Sarkar, P. Chatterjee, and A. K. Chakraborty, 'Sulfides and selenides as electrodes for dye-sensitized solar cells', in *Sulfide and Selenide Based Materials for Emerging Applications*, Elsevier, 2022, pp. 243–267.

3. F. Delgado-Vargas, A. Jiménez, and O. Paredes-López, 'Natural pigments: carotenoids, anthocyanins, and betalains—characteristics, biosynthesis, processing, and stability', *Crit. Rev. Food Sci. Nutr.*, vol. 40, no. 3, pp. 173–289, 2000.

4. R. Ranveer, B. K. Sakhale, and U. Annapure, 'Microencapsulation of Natural Pigments', *Nov. Process. Methods Plant-Based Health Foods Extr. Encapsulation Health Benefits Bioact. Compd.*, p. 163, 2023.

5. K. Sharma, V. Sharma, and S. S. Sharma, 'Dye-Sensitized Solar Cells: Fundamentals and Current Status', *Nanoscale Res. Lett.*, vol. 13, no. 1, p. 381, Nov. 2018, doi: 10.1186/s11671-018-2760-6.

6. K. E. Jasim, 'Dye sensitized solar cells-working principles, challenges and opportunities', *Sol. Cells-Dye-Sensitized Devices*, vol. 8, p. 172Ā210, 2011.

7. E. T. Bekele and Y. D. Sintayehu, 'Recent Progress, Advancements, and Efficiency Improvement Techniques of Natural Plant Pigment-Based Photosensitizers for Dye-Sensitized Solar Cells', *J. Nanomater.*, vol. 2022, 2022.

8. J. Gong, J. Liang, and K. Sumathy, 'Review on dye-sensitized solar cells (DSSCs): Fundamental concepts and novel materials', *Renew. Sustain. Energy Rev.*, vol. 16, no. 8, pp. 5848–5860, 2012.

9. R. Miles, K. Hynes, and I. Forbes, 'Photovoltaic solar cells: An overview of state-of-the-art cell development and environmental issues', *Prog. Cryst. Growth Charact. Mater.*, vol. 51, no. 1–3, pp. 1–42, 2005.

10. P. G. V. Sampaio and M. O. A. González, 'A review on organic photovoltaic cell', *Int. J. Energy Res.*, vol. 46, no. 13, pp. 17813–17828, 2022.

11. B. Srinivas, S. Balaji, M. Nagendra Babu, and Y. Reddy, 'Review on present and advance materials for solar cells', *Int. J. Eng. Res.-Online*, vol. 3, pp. 178–182, 2015.

12. N. Kant and P. Singh, 'Review of next generation photovoltaic solar cell

technology and comparative materialistic development', *Mater. Today Proc.*, vol. 56, pp. 3460–3470, 2022.

13. S. Sharma, K. K. Jain, and A. Sharma, 'Solar cells: in research and applications—a review', *Mater. Sci. Appl.*, vol. 6, no. 12, p. 1145, 2015.

14. D. J. Farrell and M. Yoshida, 'Operating regimes for second generation luminescent solar concentrators', *Prog. Photovolt. Res. Appl.*, vol. 20, no. 1, pp. 93–99, 2012.

15. O. Vigil-Galán *et al.*, 'Route towards low cost-high efficiency second generation solar cells: current status and perspectives', *J. Mater. Sci. Mater. Electron.*, vol. 26, no. 8, pp. 5562–5573, 2015.

16. W. A. Badawy, 'A review on solar cells from Si-single crystals to porous materials and quantum dots', *J. Adv. Res.*, vol. 6, no. 2, pp. 123–132, 2015.

17. D. M. Bagnall and M. Boreland, 'Photovoltaic technologies', *Energy Policy*, vol. 36, no. 12, pp. 4390–4396, 2008.

18. A. Khatibi, F. Razi Astaraei, and M. H. Ahmadi, 'Generation and combination of the solar cells: A current model review', *Energy Sci. Eng.*, vol. 7, no. 2, pp. 305–322, 2019.

19. J. Albero, J. N. Clifford, and E. Palomares, 'Quantum dot based molecular solar cells', *Coord. Chem. Rev.*, vol. 263, pp. 53–64, 2014.

20. J. Yan and B. R. Saunders, 'Third-generation solar cells: a review and comparison of polymer: fullerene, hybrid polymer and perovskite solar cells', *Rsc Adv.*, vol. 4, no. 82, pp. 43286–43314, 2014.

21. S. Ananthakumar, D. Balaji, J. Ram Kumar, and S. Moorthy Babu, 'Role of co-sensitization in dye-sensitized and quantum dot-sensitized solar cells', *SN Appl. Sci.*, vol. 1, pp. 1–46, 2019.

22. T. Markvart, 'From steam engine to solar cells: can thermodynamics guide the development of future generations of photovoltaics?', *Wiley Interdiscip. Rev. Energy Environ.*, vol. 5, no. 5, pp. 543–569, 2016.

23. J.-F. Guillemoles, T. Kirchartz, D. Cahen, and U. Rau, 'Guide for the perplexed to the Shockley–Queisser model for solar cells', *Nat. Photonics*, vol. 13, no. 8, pp. 501–505, 2019.

24. O. D. Miller, E. Yablonovitch, and S. R. Kurtz, 'Strong internal and external luminescence as solar cells approach the Shockley–Queisser limit', *IEEE J. Photovolt.*, vol. 2, no. 3, pp. 303–311, 2012.

25. S. A. Mann, R. R. Grote, R. M. Osgood Jr, A. Alu, and E. C. Garnett, 'Opportunities and limitations for nanophotonic structures to exceed the Shockley–Queisser limit', *ACS Nano*, vol. 10, no. 9, pp. 8620–8631, 2016.

26. Y. Xu, T. Gong, and J. N. Munday, 'The generalized Shockley-Queisser limit for nanostructured solar cells', *Sci. Rep.*, vol. 5, no. 1, pp. 1–9, 2015.

27. Y. Gong *et al.*, 'Ag incorporation with controlled grain growth enables 12.5% efficient kesterite solar cell with open circuit voltage reached 64.2% Shockley–Queisser limit', *Adv. Funct. Mater.*, vol. 31, no. 24, p. 2101927, 2021.

28. S. V. Boriskina and G. Chen, 'Exceeding the solar cell Shockley–Queisser limit via thermal up-conversion of low-energy photons', *Opt. Commun.*, vol. 314, pp. 71–78, 2014.

29. P. Wurfel, *Physics of solar cells*. Wiley-Vch, 2005.

30. Y. Xu, T. Gong, and J. N. Munday, 'The generalized Shockley-Queisser limit for nanostructured solar cells', *Sci. Rep.*, vol. 5, no. 1, p. 13536, 2015.

31. M. Green, 'Energy, entropy and efficiency ed T Kamiya et al Third Generation Photovoltaics', 2006.

32. A. Luque and A. Martí, 'Increasing the efficiency of ideal solar cells by photon induced transitions at intermediate levels', *Phys. Rev. Lett.*, vol. 78, no. 26, p. 5014, 1997.

33. P. Landsberg and P. Baruch, 'The thermodynamics of the conversion of radiation energy for photovoltaics', *J. Phys. Math. Gen.*, vol. 22, no. 11, p. 1911, 1989.

34. A. De Vos and H. Pauwels, 'On the thermodynamic limit of photovoltaic energy conversion', *Appl. Phys.*, vol. 25, pp. 119–125, 1981.

35. P. Wang and R. Menon, 'Simulation and optimization of 1-D periodic dielectric nanostructures for light-trapping', *Opt. Express*, vol. 20, no. 2, pp. 1849–1855, 2012.

36. C. A. Gueymard, 'Spectral effects on the transmittance, solar heat gain, and performance rating of glazing systems', *Sol. Energy*, vol. 83, no. 6, pp. 940–953, 2009.

37. S. P. Bremner, M. Y. Levy, and C. B. Honsberg, 'Limiting efficiency of an intermediate band solar cell under a terrestrial spectrum', *Appl. Phys. Lett.*, vol. 92, no. 17, 2008.

38. Z. R. Abrams, A. Niv, and X. Zhang, 'Solar energy enhancement using down-converting particles: A rigorous approach', *J. Appl. Phys.*, vol. 109, no. 11, 2011.

39. C. Wu *et al.*, 'Metamaterial-based integrated plasmonic absorber/emitter for solar thermo-photovoltaic systems', *J. Opt.*, vol. 14, no. 2, p. 024005, 2012.

40. M. Florescu *et al.*, 'Improving solar cell efficiency using photonic band-gap materials', *Sol. Energy Mater. Sol. Cells*, vol. 91, no. 17, pp. 1599–1610, 2007.

41. N.-P. Harder and P. Würfel, 'Theoretical limits of thermophotovoltaic solar energy conversion', *Semicond. Sci. Technol.*, vol. 18, no. 5, p. S151, 2003.

42. E. Rephaeli and S. Fan, 'Absorber and emitter for solar thermo-photovoltaic systems to achieve efficiency exceeding the Shockley-Queisser limit', *Opt. Express*, vol. 17, no. 17, pp. 15145–15159, 2009.

43. V. Badescu, 'An extended model for upconversion in solar cells', *J. Appl. Phys.*, vol. 104, no. 11, 2008.

44. T. Trupke, M. Green, and P. Würfel, 'Improving solar cell efficiencies by down-conversion of high-energy photons', *J. Appl. Phys.*, vol. 92, no. 3, pp. 1668–1674, 2002.

45. S. Fischer *et al.*, 'Enhancement of silicon solar cell efficiency by upconversion: Optical and electrical characterization', *J. Appl. Phys.*, vol. 108, no. 4, 2010.

46. W. Zou, C. Visser, J. A. Maduro, M. S. Pshenichnikov, and J. C. Hummelen, 'Broadband dye-sensitized upconversion of near-infrared light', *Nat. Photonics*, vol. 6, no. 8, pp. 560–564, 2012.

47. H. Ellis, 'Characterization of dye-sensitized solar cells: Components for environmentally friendly photovoltaics', 2014.

48. B. O'regan and M. Grätzel, 'A low-cost, high-efficiency solar cell based on dye-sensitized colloidal TiO2 films', *nature*, vol. 353, no. 6346, pp. 737–740, 1991.

49. R. N. Gayen, V. S. Avvaru, and V. Etacheri, 'Chapter 14 - Carbon-based integrated devices for efficient photo-energy conversion and storage', in *Carbon Based Nanomaterials for Advanced Thermal and Electrochemical Energy Storage and Conversion*, R. Paul, V. Etacheri, Y. Wang, and C.-T. Lin, Eds., in Micro and Nano Technologies. Elsevier, 2019, pp. 357–374. doi: https://doi.org/10.1016/B978-0-12-814083-3.00014-7.

50. P. Prakash *et al.*, 'Optimization, fabrication, and characterization of anthocyanin and carotenoid derivatives based dye-sensitized solar cells', *J. King Saud Univ.-Sci.*, vol. 35, no. 4, p. 102625, 2023.

51. O. Adedokun, K. Titilope, and A. O. Awodugba, 'Review on natural dye-sensitized solar cells (DSSCs)', *Int. J. Eng. Technol. IJET*, vol. 2, no. 2, pp. 34–41, 2016.

52. A. Omar, M. S. Ali, and N. Abd Rahim, 'Electron transport properties analysis of titanium dioxide dye-sensitized solar cells (TiO2-DSSCs) based natural dyes using electrochemical impedance spectroscopy concept: A review', *Sol. Energy*, vol. 207, pp. 1088–1121, 2020.

53. T. Hitosugi, N. Yamada, S. Nakao, Y. Hirose, and T. Hasegawa, 'Properties of TiO2-based transparent conducting oxides', *Phys. Status Solidi A*, vol. 207, no. 7, pp. 1529–1537, 2010.

54. K. Yoo *et al.*, 'Completely transparent conducting oxide-free and flexible dye-sensitized solar cells fabricated on plastic substrates', *ACS Nano*, vol. 9, no. 4, pp. 3760–3771, 2015.

55. M. Kokkonen *et al.*, 'Advanced research trends in dye-sensitized solar cells', *J. Mater. Chem. A*, vol. 9, no. 17, pp. 10527–10545, 2021.

56. [56] A. B. Muñoz-García *et al.*, 'Dye-sensitized solar cells strike back', *Chem. Soc. Rev.*, vol. 50, no. 22, pp. 12450–12550, 2021.

57. M. Yeoh and K. Chan, 'Recent advances in photo-anode for dye-sensitized solar cells: a review', *Int. J. Energy Res.*, vol. 41, no. 15, pp. 2446–2467, 2017.

58. H. Iftikhar, G. G. Sonai, S. G. Hashmi, A. F. Nogueira, and P. D. Lund, 'Progress on electrolytes development in dye-sensitized solar cells', *Materials*, vol. 12, no. 12, p. 1998, 2019.

59. M. Dhonde, K. Sahu, M. Das, A. Yadav, P. Ghosh, and V. V. S. Murty, 'Recent advancements in dye-sensitized solar cells; from photoelectrode to counter electrode', *J. Electrochem. Soc.*, vol. 169, no. 6, p. 066507, 2022.

60. X. Wang, B. Zhao, W. Kan, Y. Xie, and K. Pan, 'Review on low-cost counter electrode materials for dye-sensitized solar cells: effective strategy to improve photovoltaic performance', *Adv. Mater. Interfaces*, vol. 9, no. 2, p. 2101229, 2022.

61. S. CHAUDHARY, V. KUMAR, and S. KUMAR, 'A Brief Review on Natural Photosensitizer Based Dye-Sensitized Solar Cells For Photoelectric Conversion.', *Orient. J. Chem.*, vol. 39, no. 2, 2023.

62. A. S. Radwan, M. R. Elmorsy, E. Abdel-Latif, M. M. Makhlouf, and S. A. Badawy, 'Innovating dye-sensitized solar cells: Thiazole-based Co-sensitizers for enhanced photovoltaic performance with theoretical insights', *Opt. Mater.*, vol. 140, p. 113914, 2023.

63. A. V. Akimov, A. J. Neukirch, and O. V. Prezhdo, 'Theoretical insights into photoinduced charge transfer and catalysis at oxide interfaces', *Chem. Rev.*, vol. 113, no. 6, pp. 4496–4565, 2013.

64. F. W. Low and C. W. Lai, 'Recent developments of graphene-TiO2 composite nanomaterials as efficient photoelectrodes in dye-sensitized solar cells: A review', *Renew. Sustain. Energy Rev.*, vol. 82, pp. 103–125, 2018.

65. J. Bisquert, F. Fabregat-Santiago, I. Mora-Sero, G. Garcia-Belmonte, and S. Gimenez, 'Electron lifetime in dye-sensitized solar cells: theory and interpretation of measurements', *J. Phys. Chem. C*, vol. 113, no. 40, pp. 17278–17290, 2009.

66. A. Sacco, 'Electrochemical impedance spectroscopy: Fundamentals and application in dye-sensitized solar cells',

Renew. Sustain. Energy Rev., vol. 79, pp. 814–829, 2017.

67. G. Garcia-Belmonte, P. P. Boix, J. Bisquert, M. Sessolo, and H. J. Bolink, 'Simultaneous determination of carrier lifetime and electron density-of-states in P3HT: PCBM organic solar cells under illumination by impedance spectroscopy', *Sol. Energy Mater. Sol. Cells*, vol. 94, no. 2, pp. 366–375, 2010.

68. C. Longo and M.-A. De Paoli, 'Dye-sensitized solar cells: a successful combination of materials', *J. Braz. Chem. Soc.*, vol. 14, pp. 898–901, 2003.

69. A. S. Teja *et al.*, 'Optimal processing methodology for futuristic natural dye sensitized solar cells and novel applications', *Dyes Pigments*, p. 110997, 2022.

70. K. Al-Attafi *et al.*, 'Solvothermally synthesized anatase TiO2 nanoparticles for photoanodes in dye-sensitized solar cells', *Sci. Technol. Adv. Mater.*, vol. 22, no. 1, pp. 100–112, 2021.

71. E. Kouhestanian, M. Ranjbar, S. Mozaffari, and H. Salaramoli, 'Investigating the effects of thickness on the performance of ZnO-based DSSC', *Prog. Color Color. Coat.*, vol. 14, no. 2, pp. 101–112, 2021.

72. A. Kawade *et al.*, 'Comparative study of eosin-y and rose bengal sensitized SnO2-ZnO composite electrode for dye-sensitized solar cell', *ES Energy Environ.*, vol. 14, pp. 73–78, 2021.

73. S. Bykkam, D. Prasad, M. R. Maurya, K. K. Sadasivuni, and J.-J. Cabibihan, 'Comparison study of metal oxides (CeO2, CuO, SnO2, CdO, ZnO and TiO2) decked few layered graphene nanocomposites for dye-sensitized solar cells', *Sustainability*, vol. 13, no. 14, p. 7685, 2021.

74. A. Hauch and A. Georg, 'Diffusion in the electrolyte and charge-transfer reaction at the platinum electrode in dye-sensitized solar cells', *Electrochimica Acta*, vol. 46,

no. 22, pp. 3457–3466, 2001, doi: https://doi.org/10.1016/S0013-4686(01)00540-0.

75. E. Singh and H. S. Nalwa, 'Graphene-based dye-sensitized solar cells: a review', *Sci. Adv. Mater.*, vol. 7, no. 10, pp. 1863–1912, 2015.

76. K. S. Novoselov *et al.*, 'Electric Field Effect in Atomically Thin Carbon Films', *Science*, vol. 306, no. 5696, pp. 666–669, 2004, doi: 10.1126/science.1102896.

77. A. K. GEIM and K. S. NOVOSELOV, 'The rise of graphene', in *Nanoscience and Technology*, pp. 11–19. doi: 10.1142/9789814287005_0002.

78. R. R. Nair *et al.*, 'Fine structure constant defines visual transparency of graphene', *Science*, vol. 320, no. 5881, pp. 1308–1308, 2008.

79. X. Li *et al.*, 'Transfer of Large-Area Graphene Films for High-Performance Transparent Conductive Electrodes', *Nano Lett.*, vol. 9, no. 12, pp. 4359–4363, 2009, doi: 10.1021/nl902623y.

80. C. Lee, X. Wei, J. W. Kysar, and J. Hone, 'Measurement of the Elastic Properties and Intrinsic Strength of Monolayer Graphene', *Science*, vol. 321, no. 5887, pp. 385–388, 2008, doi: 10.1126/science.1157996.

81. L. Zhang, J. Liang, Y. Huang, Y. Ma, Y. Wang, and Y. Chen, 'Size-controlled synthesis of graphene oxide sheets on a large scale using chemical exfoliation', *Carbon*, vol. 47, no. 14, pp. 3365–3368, 2009, doi: https://doi.org/10.1016/j.carbon.2009.07.045.

82. J. Shen, Y. Hu, C. Li, C. Qin, M. Shi, and M. Ye, 'Layer-by-Layer Self-Assembly of Graphene Nanoplatelets', *Langmuir*, vol. 25, no. 11, pp. 6122–6128, 2009, doi: 10.1021/la900126g.

83. D. C. Elias *et al.*, 'Control of Graphene's Properties by Reversible Hydrogenation: Evidence for Graphane', *Science*, vol. 323,

no. 5914, pp. 610–613, 2009, doi: 10.1126/science.1167130.

84. R. Balog *et al.*, 'Bandgap opening in graphene induced by patterned hydrogen adsorption', *Nat. Mater.*, vol. 9, no. 4, pp. 315–319, 2010.

85. [85] M. Pumera and C. H. A. Wong, 'Graphane and hydrogenated graphene', *Chem. Soc. Rev.*, vol. 42, no. 14, pp. 5987–5995, 2013.

86. Y.-C. Wang and C.-P. Cho, 'Application of TiO2-graphene nanocomposites to photoanode of dye-sensitized solar cell', *J. Photochem. Photobiol. Chem.*, vol. 332, pp. 1–9, 2017.

87. J. D. Roy-Mayhew and I. A. Aksay, 'Graphene materials and their use in dye-sensitized solar cells', *Chem. Rev.*, vol. 114, no. 12, pp. 6323–6348, 2014.

88. C.-E. Cheng *et al.*, 'Platinum-graphene counter electrodes for dye-sensitized solar cells', *J. Appl. Phys.*, vol. 114, no. 1, p. 014503, 2013.

89. [89] A. Carella, F. Borbone, and R. Centore, 'Research progress on photosensitizers for DSSC', *Front. Chem.*, vol. 6, p. 481, 2018.

90. K. S. Gupta *et al.*, 'Effect of the anchoring group in the performance of carbazole-phenothiazine dyads for dye-sensitized solar cells', *Dyes Pigments*, vol. 113, pp. 536–545, 2015.

91. G. Richhariya, A. Kumar, P. Tekasakul, and B. Gupta, 'Natural dyes for dye sensitized solar cell: A review', *Renew. Sustain. Energy Rev.*, vol. 69, pp. 705–718, 2017.

92. A. Leite, H. da Cunha, J. Rodrigues, R. S. Babu, and A. de Barros, 'Construction and characterization of organic photovoltaic cells sensitized by Chrysanthemum based natural dye', *Spectrochim. Acta. A. Mol. Biomol. Spectrosc.*, vol. 284, p. 121780, 2023.

93. M. Alhamed, A. S. Issa, and A. W. Doubal, 'Studying of natural dyes properties as photo-sensitizer for dye sensitized solar cells (DSSC)', *J. Electron Devices*, vol. 16, no. 11, pp. 1370–1383, 2012.

94. K. Wongcharee, V. Meeyoo, and S. Chavadej, 'Dye-sensitized solar cell using natural dyes extracted from rosella and blue pea flowers', *Sol. Energy Mater. Sol. Cells*, vol. 91, no. 7, pp. 566–571, 2007.

95. S. Aghazada and M. K. Nazeeruddin, 'Ruthenium complexes as sensitizers in dye-sensitized solar cells', *Inorganics*, vol. 6, no. 2, p. 52, 2018.

96. E. Krawczak, 'Dye photosensitizers and their influence on DSSC efficiency: a review', *Inform. Autom. Pomiary W Gospod. Ochr. Śr.*, vol. 9, 2019.

97. M. K. Nazeeruddin, P. Pechy, and M. Grätzel, 'Efficient panchromatic sensitization of nanocrystallineTiO2 films by a black dye based on atrithiocyanato–ruthenium complex', *Chem. Commun.*, no. 18, pp. 1705–1706, 1997.

98. E. Abdou, H. Hafez, E. Bakir, and M. Abdel-Mottaleb, 'Photostability of low cost dye-sensitized solar cells based on natural and synthetic dyes', *Spectrochim. Acta. A. Mol. Biomol. Spectrosc.*, vol. 115, pp. 202–207, 2013.

99. S. Dayan, N. Kayaci, and N. K. Özpozan, 'Improved performance with molecular design of Ruthenium (II) complexes bearing diamine-based bidentate ligands as sensitizer for dye-sensitized solar cells (DSSC)', *J. Mol. Struct.*, vol. 1209, p. 127920, 2020.

100. J. Luo *et al.*, 'Efficient dye-sensitized solar cells based on concerted companion dyes: Systematic optimization of thiophene units in the organic dye components', *Chin. Chem. Lett.*, vol. 33, no. 9, pp. 4313–4316, 2022.

101. S. Hao, J. Wu, Y. Huang, and J. Lin, 'Natural dyes as photosensitizers for dye-sensitized solar cell', *Sol. Energy*, vol. 80, no. 2, pp. 209–214, 2006.

102.　　A. Soosairaj, A. Gunasekaran, S. Anandan, and L. R. Asirvatham, 'Synergetic effect of Leucophyllum frutescens and Ehretia microphylla dyes in enhancing the photovoltaic performance of dye-sensitized solar cells', *Environ. Sci. Pollut. Res.*, vol. 30, no. 18, pp. 52895–52905, 2023.

103.　　Z. Liu, 'Theoretical studies of natural pigments relevant to dye-sensitized solar cells', *J. Mol. Struct. THEOCHEM*, vol. 862, no. 1–3, pp. 44–48, 2008.

104.　　[104] U. Mehmood, S. Rahman, K. Harrabi, I. A. Hussein, and B. Reddy, 'Recent advances in dye sensitized solar cells', *Adv. Mater. Sci. Eng.*, vol. 2014, 2014.

105.　　E. Młodzińska, 'Survey of plant pigments: molecular and environmental determinants of plant colors', *Acta Biol. Cracovienca Ser. Bot.*, vol. 51, no. 1, pp. 7–16, 2009.

106.　　S. Shalini, S. Prasanna, T. K. Mallick, and S. Senthilarasu, 'Review on natural dye sensitized solar cells: Operation, materials and methods', *Renew. Sustain. Energy Rev.*, vol. 51, pp. 1306–1325, 2015.

107.　　E. Wong, 'The role of chalcones and flavanones in flavonoid biosynthesis', *Phytochemistry*, vol. 7, no. 10, pp. 1751–1758, 1968.

108.　　N. A. Ludin, A. A.-A. Mahmoud, A. B. Mohamad, A. A. H. Kadhum, K. Sopian, and N. S. A. Karim, 'Review on the development of natural dye photosensitizer for dye-sensitized solar cells', *Renew. Sustain. Energy Rev.*, vol. 31, pp. 386–396, 2014.

109.　　A. Zdyb and S. Krawczyk, 'Natural flavonoids as potential photosensitizers for dye-sensitized solar cells', *Ecol. Chem. Eng. S*, vol. 26, no. 1, pp. 29–36, 2019.

110.　　O. Adedokun, K. Titilope, and A. O. Awodugba, 'Review on natural dye-sensitized solar cells (DSSCs)', *Int. J. Eng.*

Technol. IJET, vol. 2, no. 2, pp. 34–41, 2016.

111.　　M. Khalili, M. Abedi, and H. S. Amoli, 'Influence of saffron carotenoids and mulberry anthocyanins as natural sensitizers on performance of dye-sensitized solar cells', *Ionics*, vol. 23, pp. 779–787, 2017.

112.　　Y. Koyama, Y. Kakitani, and H. Nagae, 'Mechanisms of suppression and enhancement of photocurrent/conversion efficiency in dye-sensitized solar-cells using carotenoid and chlorophyll derivatives as sensitizers', *Molecules*, vol. 17, no. 2, pp. 2188–2218, 2012.

113.　　P. Prakash *et al.*, 'Optimization, fabrication, and characterization of anthocyanin and carotenoid derivatives based dye-sensitized solar cells', *J. King Saud Univ.-Sci.*, vol. 35, no. 4, p. 102625, 2023.

114.　　A. Singh and T. Mukherjee, 'Application of carotenoids in sustainable energy and green electronics', *Mater. Adv.*, vol. 3, no. 3, pp. 1341–1358, 2022.

115.　　A. Supriyanto, F. Nurosyid, and A. Ahliha, 'Carotenoid pigment as sensitizers for applications of dye-sensitized solar cell (DSSC)', presented at the IOP Conference Series: Materials Science and Engineering, IOP Publishing, 2018, p. 012060.

116.　　X.-F. Wang, Y. Koyama, Y. Wada, S. Sasaki, and H. Tamiaki, 'A dye-sensitized solar cell using pheophytin–carotenoid adduct: Enhancement of photocurrent by electron and singlet-energy transfer and by suppression of singlet–triplet annihilation due to the presence of the carotenoid moiety', *Chem. Phys. Lett.*, vol. 439, no. 1–3, pp. 115–120, 2007.

117.　　E. Yamazaki, M. Murayama, N. Nishikawa, N. Hashimoto, M. Shoyama, and O. Kurita, 'Utilization of natural carotenoids as photosensitizers for dye-

sensitized solar cells', *Sol. Energy*, vol. 81, no. 4, pp. 512–516, 2007.

118. H. Hug, M. Bader, P. Mair, and T. Glatzel, 'Biophotovoltaics: natural pigments in dye-sensitized solar cells', *Appl. Energy*, vol. 115, pp. 216–225, 2014.

119. N. Y. Amogne, D. W. Ayele, and Y. A. Tsigie, 'Recent advances in anthocyanin dyes extracted from plants for dye sensitized solar cell', *Mater. Renew. Sustain. Energy*, vol. 9, pp. 1–16, 2020.

120. G. Takeoka and L. Dao, 'Anthocyanins', *Methods Anal. Funct. Foods Nutraceuticals*, vol. 1, 2002.

121. W. Steyn, S. Wand, D. Holcroft, and G. Jacobs, 'Anthocyanins in vegetative tissues: a proposed unified function in photoprotection', *New Phytol.*, vol. 155, no. 3, pp. 349–361, 2002.

122. S. C. Ezike, C. N. Hyelnasinyi, M. A. Salawu, J. F. Wansah, A. N. Ossai, and N. N. Agu, 'Synergestic effect of chlorophyll and anthocyanin Co-sensitizers in TiO2-based dye-sensitized solar cells', *Surf. Interfaces*, vol. 22, p. 100882, 2021.

123. R. Ramamoorthy, N. Radha, G. Maheswari, S. Anandan, S. Manoharan, and R. Victor Williams, 'Betalain and anthocyanin dye-sensitized solar cells', *J. Appl. Electrochem.*, vol. 46, pp. 929–941, 2016.

124. V. Pramananda, T. A. H. Fityay, and E. Misran, 'Anthocyanin as natural dye in DSSC fabrication: A review', presented at the IOP Conference Series: Materials Science and Engineering, IOP Publishing, 2021, p. 012104.

125. G. F. C. Mejica, Y. Unpaprom, D. Balakrishnan, N. Dussadee, S. Buochareon, and R. Ramaraj, 'Anthocyanin pigment-based dye-sensitized solar cells with improved pH-dependent photovoltaic properties', *Sustain. Energy Technol. Assess.*, vol. 51, p. 101971, 2022.

126. X.-F. Wang, O. Kitao, E. Hosono, H. Zhou, S. Sasaki, and H. Tamiaki, 'TiO2-and ZnO-based solar cells using a chlorophyll a derivative sensitizer for light-harvesting and energy conversion', *J. Photochem. Photobiol. Chem.*, vol. 210, no. 2–3, pp. 145–152, 2010.

127. R. Barragán, M. Strojnik, A. Rodríguez-Rivas, G. G. Torales, and F. J. González, 'Optical spectral characterization of leaves for Quercus Resinosa and Magnolifolia species in two senescent states', presented at the Infrared Remote Sensing and Instrumentation XXVI, SPIE, 2018, pp. 234–242.

128. M. Abdullah *et al.*, 'Synergistic effect of complementary organic dye co-sensitizers for potential panchromatic light-harvesting of dye-sensitized solar cells', *Opt. Mater.*, vol. 133, p. 113016, 2022.

129. A. S. Teja *et al.*, 'Synergistic co-sensitization of environment-friendly chlorophyll and anthocyanin-based natural dye-sensitized solar cells: An effective approach towards enhanced efficiency and stability', *Sol. Energy*, vol. 261, pp. 112–124, 2023.

130. D. J. Godibo, S. T. Anshebo, and T. Y. Anshebo, 'Dye sensitized solar cells using natural pigments from five plants and quasi-solid state electrolyte', *J. Braz. Chem. Soc.*, vol. 26, pp. 92–101, 2015.

131. B. L. Sampaio, R. Edrada-Ebel, and F. B. Da Costa, 'Effect of the environment on the secondary metabolic profile of Tithonia diversifolia: a model for environmental metabolomics of plants', *Sci. Rep.*, vol. 6, no. 1, pp. 1–11, 2016.

132. W. Zhou, Z. Yuan, G. Li, J. Ouyang, Y. Suo, and H. Wang, 'Isolation and structure determination of a new flavone glycoside from seed residues of seabuckthorn (Hippophae rhamnoides L.)',

Nat. Prod. Res., vol. 32, no. 8, pp. 892–897, 2018.

133.   V. Pandey, A. Patel, and D. Patra, 'Amelioration of mineral nutrition, productivity, antioxidant activity and aroma profile in marigold (Tagetes minuta L.) with organic and chemical fertilization', *Ind. Crops Prod.*, vol. 76, pp. 378–385, 2015.

134.   I. Shahzadi and M. M. Shah, 'Acylated flavonol glycosides from Tagetes minuta with antibacterial activity', *Front. Pharmacol.*, vol. 6, p. 195, 2015.

135.   T. D. Xuan and T. D. Khanh, 'Chemistry and pharmacology of Bidens pilosa: an overview', *J. Pharm. Investig.*, vol. 46, no. 2, pp. 91–132, 2016.

136.   W.-C. Lee, C.-C. Peng, C.-H. Chang, S.-H. Huang, and C.-C. Chyau, 'Extraction of antioxidant components from Bidens pilosa flowers and their uptake by human intestinal Caco-2 cells', *Molecules*, vol. 18, no. 2, pp. 1582–1601, 2013.

137.   S. Mtambo, S. Krishna, and P. Govender, 'Physico-chemical, antimicrobial and anticancer properties of silver nanoparticles synthesised from organ-specific extracts of Bidens pilosa L.', *South Afr. J. Bot.*, vol. 126, pp. 196–206, 2019.

138.   S. E. Koops, B. C. O'Regan, P. R. Barnes, and J. R. Durrant, 'Parameters influencing the efficiency of electron injection in dye-sensitized solar cells', *J. Am. Chem. Soc.*, vol. 131, no. 13, pp. 4808–4818, 2009.

139.   Z. Yi *et al.*, 'Synthesis, surface properties, crystal structure and dye-sensitized solar cell performance of TiO2 nanotube arrays anodized under different parameters', *Results Phys.*, vol. 15, p. 102609, 2019.

140.   R. Ramamoorthy *et al.*, 'Reduced graphene oxide embedded titanium dioxide nanocomposite as novel photoanode material in natural dye-sensitized solar cells', *J. Mater. Sci. Mater. Electron.*, vol. 28, no. 18, pp. 13678–13689, 2017.

141.   L. Qiu, H. Zhang, W. Wang, Y. Chen, and R. Wang, 'Effects of hydrazine hydrate treatment on the performance of reduced graphene oxide film as counter electrode in dye-sensitized solar cells', *Appl. Surf. Sci.*, vol. 319, pp. 339–343, 2014.

142.   S. Sowmya, P. Prakash, N. Ruba, B. Janarthanan, A. Nagamani Prabu, and J. Chandrasekaran, 'A study on the fabrication and characterization of dye-sensitized solar cells with Amaranthus red and Lawsonia inermis as sensitizers with maximum absorption of visible light', *J. Mater. Sci. Mater. Electron.*, vol. 31, no. 8, pp. 6027–6035, 2020.

143.   A. Omar, M. S. Fakir, K. S. Hamdan, N. H. Rased, and N. A. Rahim, 'Chemical, optical and photovoltaic properties of TiO2/reduced graphene oxide photoanodes sensitized with Roselle and N719 dyes for dye-sensitized solar cell application', *Pigment Resin Technol.*, 2020.

144.   W. Ghann *et al.*, 'Fabrication, optimization and characterization of natural dye sensitized solar cell', *Sci. Rep.*, vol. 7, no. 1, pp. 1–12, 2017.

145.   W. E. Ghann *et al.*, 'Synthesis and characterization of reduced graphene oxide and their application in dye-sensitized solar cells', *ChemEngineering*, vol. 3, no. 1, p. 7, 2019.

146.   A. M. Ammar, H. S. Mohamed, M. M. Yousef, G. M. Abdel-Hafez, A. S. Hassanien, and A. S. Khalil, 'Dye-sensitized solar cells (DSSCs) based on extracted natural dyes', *J. Nanomater.*, vol. 2019, 2019.

147.   A. Pervez *et al.*, 'Fabrication and comparison of dye-sensitized solar cells by using TiO2 and ZnO as photo electrode', *Optik*, vol. 182, pp. 175–180, 2019.

148. K.-C. Cho, H. Chang, C.-H. Chen, M.-J. Kao, and X.-R. Lai, 'A study of mixed vegetable dyes with different extraction concentrations for use as a sensitizer for dye-sensitized solar cells', *Int. J. Photoenergy*, vol. 2014, 2014.

149. K. Maabong *et al.*, 'Natural pigments as photosensitizers for dye-sensitized solar cells with TiO2 thin films', *Int. J. Renew. Energy Res. IJRER*, vol. 5, no. 2, pp. 501–506, 2015.

150. D. Kuang, C. Klein, H. J. Snaith, R. Humphry-Baker, S. M. Zakeeruddin, and M. Grätzel, 'A new ion-coordinating ruthenium sensitizer for mesoscopic dye-sensitized solar cells', *Inorganica Chim. Acta*, vol. 361, no. 3, pp. 699–706, 2008.

151. Y. Qin and Q. Peng, 'Ruthenium sensitizers and their applications in dye-sensitized solar cells', *Int. J. Photoenergy*, vol. 2012, 2012.

152. S.-H. Nam, K. H. Lee, J.-H. Yu, and J.-H. Boo, 'Review of the development of dyes for dye-sensitized solar cells', *Appl. Sci. Converg. Technol.*, vol. 28, no. 6, pp. 194–206, 2019.

153. S. Mathew *et al.*, 'Dye-sensitized solar cells with 13% efficiency achieved through the molecular engineering of porphyrin sensitizers', *Nat. Chem.*, vol. 6, no. 3, pp. 242–247, 2014.

154. W. C. Oh, K. Y. Cho, C. H. Jung, and Y. Areerob, 'Hybrid of graphene based on quaternary Cu2ZnNiSe4–WO3 nanorods for counter electrode in dye-sensitized solar cell application', *Sci. Rep.*, vol. 10, no. 1, p. 4738, 2020.

155. Q. Pang, L. Leng, L. Zhao, L. Zhou, C. Liang, and Y. Lan, 'Dye sensitized solar cells using freestanding TiO2 nanotube arrays on FTO substrate as photoanode', *Mater. Chem. Phys.*, vol. 125, no. 3, pp. 612–616, 2011.

156. X. Mao *et al.*, 'High efficiency dye-sensitized solar cells constructed with composites of TiO2 and the hot-bubbling synthesized ultra-small SnO2 nanocrystals', *Sci. Rep.*, vol. 6, no. 1, p. 19390, 2016.

157. J. A. Mikroyannidis, M. M. Stylianakis, M. Roy, P. Suresh, and G. Sharma, 'Synthesis, photophysics of two new perylene bisimides and their photovoltaic performances in quasi solid state dye sensitized solar cells', *J. Power Sources*, vol. 194, no. 2, pp. 1171–1179, 2009.